

MODELLING OF TRITIUM BREEDING IN MOLTEN SALT REACTORS

MODELLING OF TRITIUM BREEDING IN MOLTEN SALT REACTORS

By HADEEL AL-ZUBAIDI, B.ENG.

A Thesis Submitted to the School of Graduate Studies in Partial Fulfilment of the
Requirements for the Degree Master of Applied Science

McMaster University © Copyright by Hadeel Al-Zubaidi, November 2023

Abstract

Nuclear fusion is considered a clean energy source: it emits no CO₂ and leaves little radioactive waste. It is important to start paving the path toward nuclear fusion whilst simultaneously moving away from fossil fuels and carbon emissions.

One of the challenges of nuclear fusion is the lack of tritium, which, together with deuterium makes up its fuel. This research is focused on utilizing one current method of nuclear fission technology, namely molten salt reactors, to generate at least the initial loads of tritium for the first fusion reactors.

Current research is primarily focused on providing tritium during the nuclear fusion reaction. However, it is also necessary to have a tritium supply whenever we start up a nuclear fusion reactor.

The largest source of tritium is the CANDU nuclear fission reactor. A typical 500 MW CANDU produces 130 g of tritium annually [1] as a byproduct of power generation. However, a future commercial fusion power plant is expected to consume 300 g of tritium per day to produce 800 MW [2].

Thus, this research explores the possibility of breeding tritium in other fission reactors, in particular molten salt reactors (MSR).

MCNP4C was used to simulate a simple Molten Salt Reactor setting with 61 molten salt fuel channels and applying a molten salt blanket to study how the

presence of specific elements in the blanket affects tritium production, as well as criticality.

The study relies on nuclear data from the National Nuclear Data Center (NNDC), and Oak Ridge National Laboratory (ORNL) as benchmark to verify the accuracy of the results.

The calculated output of tritium is 325 g/year for a 100 MW (th) reactor, which is considered a positive outcome that opens the door for more research in this direction.

Acknowledgement

I would like to acknowledge and give my warmest thanks to my supervisor at McMaster University, Dr. Adriaan Buijs, who made this work possible. His continuous guidance and advice carried me through all the stages of writing this thesis.

I would also like to take the opportunity, to say thank you for the support I received from all the nuclear engineering professors at McMaster University.

On a personal level, I received tremendous support from my family, and I would like to give a special mention to the memory of my parents, who shaped me despite their early departure from my life. Their memory gave me strength through my difficult journey as a refugee. Ahmed Alwan Hassoun Al-Zubaidi, my father, the historian, who was always proud to teach me about Sumerian civilization and Fawzia Ali Hussein Al-Hasani, my mother, the particle physics professor, who was also my teacher and friend, and who showed me that the path of knowledge is the most rewarding path.

Table of Contents

TABLE OF CONTENTS	VI
LIST OF FIGURES	X
LIST OF TABLES	XIII
LIST OF ABBREVIATIONS AND SYMBOLS	XIV
DECLARATION OF ACADEMIC ACHIEVEMENT	XV
INTRODUCTION.....	1
CHAPTER 1 NUCLEAR ENERGY – THEORETICAL REVIEW	3
1.1 NUCLEAR BINDING ENERGY.....	3
<i>1.1.1 Liquid Drop Model</i>	<i>3</i>
<i>1.1.2 Example fission of ²³⁵U vs Fusion of two deuterium nuclei.....</i>	<i>6</i>
1.2 NUCLEAR RADIOACTIVITY	7
<i>1.2.1 Spontaneous fission and/or ejecting alpha particles (α)</i>	<i>9</i>
<i>1.2.2 Beta (β) decay.....</i>	<i>9</i>
<i>1.2.3 Gamma decay (γ)</i>	<i>10</i>
1.3 NUCLEAR FISSION	11
<i>1.3.1 Neutron interaction with matter.</i>	<i>12</i>
<i>1.3.2 Controlled Fission Reaction.....</i>	<i>16</i>
<i>1.3.3 Nuclear Fission Reactor Types.....</i>	<i>22</i>
1.4 NUCLEAR FUSION	25

1.4.1	<i>Nuclear Fusion Requirements</i>	28
1.4.2	<i>Methods of Nuclear Fusion Confinement</i>	37
1.4.3	<i>Nuclear Fusion Fuel</i>	40
CHAPTER 2 TRITIUM BREEDING		41
2.1	TRITIUM ISSUE	41
2.2	ROLE OF LITHIUM IN TRITIUM PRODUCTION	42
2.3	ROLE OF BERYLLIUM IN TRITIUM PRODUCTION	44
2.4	ROLE OF LEAD IN TRITIUM PRODUCTION	44
2.5	CONCURRENT TRITIUM BREEDING RESEARCH	45
2.5.1	<i>The LIBRA Experiment</i>	45
2.5.2	<i>ITER Tritium Breeding Module</i>	48
2.6	ROLE OF MOLTEN SALT REACTOR	50
CHAPTER 3 METHODOLOGY		52
3.1	MSR, GENERAL INTRODUCTION	52
3.1.1	<i>MSRE's Fuel and Coolant Mixture</i>	52
3.1.2	<i>Neutron Economy and the Choice of Salt</i>	53
3.1.3	<i>Lithium in MSRE</i>	54
3.2	MCNP4C	56
3.3	METHOD	56
3.3.1	<i>Experiment Setting and Design</i>	56
3.3.2	<i>The Process</i>	58

CHAPTER 4 RESULTS AND VERIFICATION	61
4.1 INTRODUCTION – MCNP4C DATA COLLECTION TOOLS	61
4.2 DATA COLLECTION AND OBSERVATION	61
4.2.1 <i>Stage 1 – Finding the optimal thickness.</i>	61
4.2.2 <i>Stage 2 – Effect of ⁶Li enrichment in a fixed thickness in the blanket</i>	63
4.2.3 <i>Data summary and observations</i>	65
4.3 VERIFICATION AND BENCHMARKING	65
4.3.1 <i>Identifying ⁶Li cross section using MCNP4C</i>	65
4.3.2 <i>Benchmarking – Comparison with ORNL results.</i>	68
4.3.3 <i>Verification Summary</i>	69
CHAPTER 5 CONCLUSION AND RECOMMENDATION.....	70
5.1 CONCLUSION	70
5.2 RECOMMENDATION	71
APPENDIX A ELEMENTS CLASSIFICATION AND RADIOACTIVITY	72
A. 1 PERIODIC TABLE.	72
A. 2 RADIOACTIVITY MEASUREMENT	73
APPENDIX B DATA AND MCNP4C CODE SAMPLES	76
B. 1 INPUT FILE EXAMPLE.....	76
B. 2 OUTPUT FILE EXAMPLE.....	78
B. 3 VERIFICATION ⁶ LI TEST OUTPUT	79
B. 4 BENCHMARKING WITH ORNL.....	80

APPENDIX C USEFUL CONSTANTS, AND USEFUL MATHEMATICS 84

C. 1 CONSTANTS, MASSES AND CONVERSION FACTORS 84

C. 2 MAXWELL-BOLTZMANN DISTRIBUTION..... 85

C. 3 USEFUL MATHEMATICS..... 86

REFERENCES..... 87

List of Figures

FIGURE 1.1. BINDING ENERGY PER NUCLEON AS A FUNCTION OF MASS NUMBER A [3]-(SEC 2.3).....	6
FIGURE 1.2. SEGRÈ CHART FOR STABLE AND UNSTABLE NUCLEI [3]-(2.4).....	8
FIGURE 1.3. NEUTRON INCIDENT ON A TARGET.	15
FIGURE 1.4. DISTRIBUTION OF PROMPT NEUTRONS ENERGY AFTER ^{235}U FISSION REACTION [4]-(SEC 3-4).....	17
FIGURE 1.5. CROSS SECTION FOR NEUTRON-INDUCED FISSION OF ^{235}U AND ^{238}U [7].....	18
FIGURE 1.6. TOTAL AND FISSION CROSS SECTION OF ^{232}Th AND FISSION CROSS SECTION OF ^{233}U [7].	20
FIGURE 1.7. TOTAL AND FISSION CROSS SECTION OF ^{238}U AND FISSION CROSS SECTION OF ^{239}Pu [7].....	21
FIGURE 1.8. SCHEMATIC DIAGRAM CANDU [5]-(SEC 13.6).....	23
FIGURE 1.9. AN MSR SCHEMATIC [8].....	25
FIGURE 1.10..TRITIUM IONS BEAM HITTING A DEUTERIUM ICE-CUBE [9]-(SEC 1.5.1).	28
FIGURE 1.11. FUSION CHAIN REACTION ON THE SUN [10].	29
FIGURE 1.12. THE CROSS-SECTION OF D-T, D- ^3He AND D-D FUSION REACTIONS [9]-(SEC 1.5).....	30
FIGURE 1.13. LAWSON’S CRITERION [9]-(SEC 4.4.2.3).....	37

FIGURE 1.14. PRINCIPLE OF TOKAMAK METHOD OF MAGNETIC CONFINEMENT [5].	38
FIGURE 1.15. INERTIAL CONFINEMENT FUSION PRINCIPALE [9].	39
FIGURE 1.16. SCHEMATIC OF A NIF IGNITION TARGET. THE FUEL CAPSULE IS SUSPENDED INSIDE GOLD OR ANOTHER HIGH-Z [13].	40
FIGURE 2.1. ENERGY THRESHOLD AND CROSS SECTION OF ^{14}N INTERACTION WITH NEUTRON [7].	42
FIGURE 2.2. CROSS SECTION FOR NEUTRON INTERACTION AS A FUNCTION OF ENERGY FOR ^7Li , ^6Li , ^9Be AND Pb [7].	43
FIGURE 2.3. ARC SCHEMATIC [19].	46
FIGURE 2.4. (A) A D-T NEUTRON GENERATOR IS SURROUNDED BY A CYLINDRICAL TANK OF FLiBe ($\sim 1\text{M}$ DIAMETER). (B) TRITIUM IS CARRIED TO THE DETECTION SYSTEM VIA THE COVER GAS OR VIA LINER SWEEP GAS RETURN. (C) LIBRA PROCESS [18].	47
FIGURE 2.5. (A) SCHEMATIC OF THE CYLINDRICAL LIB CROSS-SECTION. (B) RMS DEVIATION IN NEUTRON ENERGY SPECTRA IS PLOTTED AS A FUNCTION OF FLiBe THICKNESS. (C) LIBRA TBR IS PLOTTED AS A FUNCTION OF FLiBe THICKNESS [18].	48
FIGURE 2.6. HCCB TBS DESIGN OPTIMIZATION OF THE TBM [20].	49
FIGURE 2.7. NORMALIZED NEUTRON ENERGY SPECTRA FOR DD, TT, AND DT FUSION [21].	50
FIGURE 3.1. LiF-BEF2 DILUENT SYSTEM [23].	53

FIGURE 3.2. REDOX POTENTIALS OF VARIOUS REDOX COUPLES AS A FUNCTION OF TEMPERATURE IN FLUORIDE SALTS. SOLID LINE: METAL DISSOLUTION. DOTTED LINE: REDUCTION OF OXIDANTS [24].	55
FIGURE 3.3. CROSS SECTION OF SIMPLE MOLTEN SALT REACTOR ARRANGEMENT. FIGURE CREATED USING MCNP4C.	57
FIGURE 4.1. DATA BASED ON MCNP4C OUTPUT FOR FOUR BLANKET THICKNESS/PROPORTIONAL ${}^6\text{Li}$ ENRICHMENT.	63
FIGURE 4.2. DATA BASED ON MCNP4C OUTPUT FOR DIFFERENT ${}^6\text{Li}$ ENRICHMENT LEVEL IN THE BLANKET.	64
FIGURE 4.3. TEST CELL. A TEST WAS RUN FOR EACH LISTED ENERGY LEVEL.	66
FIGURE 4.4. ${}^6\text{Li}$ CROSS SECTION AS CALCULATED USING MCNP4C, AND RELATIVE ERROR.	67
FIGURE 4.5. TOP VIEW CROSS SECTION OF SIMPLE MOLTEN SALT REACTOR ARRANGEMENT FOR ORNL BENCHMARKING. FIGURE CREATED USING MCNP4C.	68
FIGURE A. 1. PERIODIC TABLE [30].	72
FIGURE C. 1. SPEED DISTRIBUTION FUNCTION (MAXWELL-BOLTZMANN DISTRIBUTION) [11]-(SEC 5.2).	86

List of Tables

TABLE 1.1. BINDING ENERGY CALCULATION FOR ^{235}U AND ITS FISSION PRODUCT. -	6
TABLE 1.2 NEUTRON ENERGY CLASSIFICATION -----	13
TABLE 3.1. MSRE MOLTEN SALT FUEL MIXTURE [23]. -----	52
TABLE 3.2. ORNL MOLTEN SALT SECONDARY COOLANT MIXTURE [23]. -----	53
TABLE 3.3. EXPERIMENT MOLTEN SALT FUEL MIXTURE.-----	58
TABLE 3.4. EXPERIMENT FUEL MIX – ELEMENTS WEIGHT DISTRIBUTION PER 1 GRAM. -----	59
TABLE 4.1. MCNP4C FILES WITH BLANKET THICKNESS, AND ^6Li OPTIMAL LEVEL ENRICHMENT. -----	62
TABLE 4.2. BLANKET 20 CM THICKNESS - ELEMENTS WEIGHT DISTRIBUTION PER 1 GRAM. -----	62
TABLE 4.3. MCNP4C FILE WITH VARIABLE ^6Li ENRICHMENT. -----	64
TABLE 4.4. ^6Li CROSS SECTION AT SPECIFIC NEUTRON ENERGY FROM NNDC. -----	66

List of Abbreviations and Symbols

ARC	Affordable, Robust, and Compact
CANDU	Canada Deuterium Uranium
CNSC	Canadian Nuclear Safety Commission
ENDF	Evaluated Nuclear Data File
IAEA	International Atomic Energy Agency
ICF	Inertial Confinement Fusion
ITER	International Thermonuclear Experiment Reactor
JET	Joint European Tokamak
LIBRA	Liquid Immersion Blanket: Robust Accountancy
MCNP	Monte Carlo N-Particle
MSR	Molten Salt Reactor
MSRE	Molten Salt Reactor Experiment
NIF	National Ignition Facility
NNDC	National Nuclear Data Center
ORNL	Oak Ridge National Laboratory
Redox	Oxidization Reduction
TBR	Tritium Breeding Ration

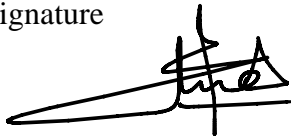
Declaration of Academic Achievement

I, Hadeel Al-Zubaidi, declare that this thesis titled “MODELLING OF TRITIUM BREEDING IN MOLTEN SALT REACTORS” to be my own work. I am the author of this document. No part of this work has been submitted for any degree, diploma, associateship, fellowship, or other similar title of any other university or institution.

To the best of my knowledge, the content of this document does not infringe on anyone’s copyright.

My supervisor, Dr Adriaan Buijs, has provided guidance and support at all stages of this project.

Signature

A handwritten signature in black ink, appearing to be 'Hadeel Al-Zubaidi', written over a horizontal line.

Date

November 16, 2023

Introduction

Since the dawn of civilization, energy has been at the core of any improvement to human lives. It began with the discovery of fire. Since then, sources of energy have evolved, but without that first flame, we would never have achieved the standards of life we see today.

Today, energy is one of the primary global concerns because of its close relationships with both quality of life and the environment. The current world focus is on moving away from fossil fuels and reducing carbon footprint in order to combat climate change.

Nuclear fusion would enable us to meet this demand and is the ultimate goal of this research.

However, fusion, as we will see in the coming chapters, has multiple barriers, among them the lack of tritium. The primary purpose of this specific study is to secure a continuous supply of tritium to ensure not only sufficient fuel for startup of fusion reactions, but also enough tritium to further research into improving nuclear fusion technology. Current research projects are focused on maintaining tritium production once a fusion reaction is in progress, but there is a shortage of tritium for starting up such reactions. This study will examine the feasibility of using existing nuclear fission technology, in this case a molten salt reactor, to

purposefully breed tritium to both further research into, and provide fuel for, nuclear fusion projects.

Chapter 1

Nuclear energy – Theoretical review

Nuclear energy comes from the smallest unit of matter, the nucleus. *Albert Einstein's* formula equation (1.1) relates mass to energy in one simple equation.

$$E = mc^2 \quad (1.1)$$

This chapter will show how this concept leads to nuclear fission and fusion energy.

1.1 Nuclear Binding Energy.

The nucleus consists of Z protons and N neutrons. Z gives the element its identity and place in the periodic table, whereas $A = N+Z$ represents the atomic mass number. Nuclear energy relies on releasing some of the inner energy that binds A nucleons within a nucleus, by either splitting the nucleus and releasing multiple nuclei – fission, or by fusing two nuclei together – fusion.

1.1.1 Liquid Drop Model

Aside from the lightest elements, the binding energy for most nuclei ($A > 20$) is well explained mathematically with the liquid drop model [3]-(Sec 2.3). According to this model,

- a) The average number of nucleons per unit volume in a nucleus is constant for all nuclei [4]-(Sec1-3). Thus, to identify the volume, the atomic nucleus can be approximated according to equation (1.2) [3]-(Sec 2.2).

$$R = 1.21A^{1/3} \text{ [fm]} \quad (1.2)$$

Where R is called the *effective radius* [3]-(Sec 2.2), and the constant 1.21 is an approximated value derived from neutron scattering experiments, [4]-(Sec 1-3). hence the total binding energy of any nucleus is proportional to its mass number A [3]-(Sec 2.3).

- b) Since the nucleons at the surface are not surrounded by other nucleons, this will lower the average binding energy in proportion to the surface area [3]-(Sec 2.3).
- c) As Z increases, the coulomb repulsive forces increase, thus lowering the binding energy proportionally to Z^2 [3]-(Sec 2.3).
- d) Stable nuclei have the tendency of having $Z \approx N$, but as the size of the nuclei increase, the Coulomb repulsion also increases, therefore more neutrons are needed for nuclear stability [3]-(Sec 2.3).
- e) The parity between the neutrons and protons is dependent on the number of Z and N . It is negative if both Z and N are odd, positive if both Z and N are even, and zero otherwise [3]-(Sec 2.3).

Thus, the liquid drop model is interpreted mathematically using the semi-empirical formula (1.3) below [3]-(Sec 2.3) & [5]-(Sec 3.3),

$$E_B = a_v A - a_s A^{2/3} - a_c \frac{Z^2}{A^{1/3}} - a_{sym} \frac{(A - 2Z)^2}{A} \mp a_p A^{-1/2} \quad (1.3)$$

Where E_B is the total binding energy, the coefficient a_v , a_s , a_c , a_{sym} and a_p values are calculated according to the fitting method used to get the best agreement with the experimental curve shown in **Figure 1.1**. A set often used [3]-(Sec 2.3) is, in units of [MeV]:

$$a_v = 15.56, \quad a_s = 17.23, \quad a_c = 0.697, \quad a_{sym} = 23.3, \quad a_p = 12 \quad (1.4)$$

Figure 1.1 shows the curve of the average binding energy per nucleon, which increases, until it reaches 56 nucleons (^{56}Fe). After that the average binding energy gradually decreases as the size increases. This figure indicates that we can generate energy in two ways [5]-(Ch 13 & 14): a) by combining two light nuclei like hydrogen (fusion), or b) by breaking a heavy nucleus like uranium or plutonium into two or more lighter nuclei (fission). In either way nuclear energy is released as we climb up the curve of binding energy. However, the slope of the curve for $A < 56$ is much bigger than the slope for $A > 56$, which means the energy released for fusion is much more than that for fission per kg of fuel used as presented in the example below.

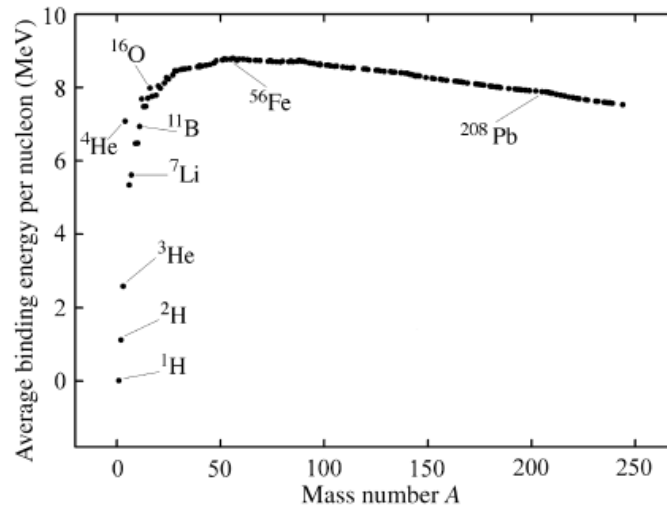


Figure 1.1. Binding energy per nucleon as a function of mass number A [3]-(Sec 2.3).

1.1.2 Example fission of ^{235}U vs Fusion of two deuterium¹ nuclei

In the case of ^{235}U fission, the mass number A of the fission product will be on Average (140, 95) and the atomic number Z is (56, 36) respectively (see Sec 1.2).

Then we can estimate the energy release per one ^{235}U nuclei using E_B formula and according to **Error! Reference source not found.**

Table 1.1. Binding energy calculation for ^{235}U and its fission product.

	$^{235}_{92}\text{U}$	$^{141}_{55}\text{Cs}$	$^{93}_{37}\text{Rb}$
Volume term	3657	2194	1447
Surface term	-656	-467	-354
Coulomb term	-956	-405	-211
Symmetry term	-258	-159	-90
Pairing term	0	0	0
Total E_B	1787	1163	792
E_B per nucleon	7.6	8.25	8.52

¹ Deuterium is a hydrogen isotope that can be written as (^2H or D)

Thus, the energy released in MeV per one ^{235}U nucleus is:

$$E_{235\text{U}} = \left(\left(\frac{8.25 \times 141 + 8.52 \times 93}{234} \right) - 7.6 \right) \times 235 \approx 180 \quad (1.5)$$

For 1 kg of ^{235}U . The energy released in Joules, is:

$$\begin{aligned} E_{1\text{ kg of }^{235}\text{U}} &= \frac{1000 [\text{g}]}{235[\text{g}]} \times N_A \times 1.6 \times 10^{-13} [\text{J}] \times 180 \\ &= 73.8 \times 10^6 \text{ MJ}, \quad N_A = 6.022 \times 10^{23} \end{aligned} \quad (1.6)$$

Where N_A is the Avogadro's Number.

For deuterium and helium ($A < 20$), the binding energy can be estimated from the experimental curve. For deuterium $E_B = 1$ MeV, for helium $E_B = 7$ MeV. The energy release in MeV per fusing two deuterium nuclei, is $(7 - 1) \times 4 = 24$ MeV. Thus, for 1 kg of deuterium, the expected energy outcome in Joule is:

$$\begin{aligned} E_{1\text{ kg of }^2\text{H}} &= \frac{1000 [\text{g}]}{2 \times 2[\text{g}]} \times N_A \times 1.6 \times 10^{-13} [\text{J}] \times 24 \\ &= 578 \times 10^6 [\text{MJ}] \end{aligned} \quad (1.7)$$

Thus, fusion produces about eight times the energy produced by fission per kg of matter.

1.2 Nuclear Radioactivity

Neutrons with a mass of $939.6 \text{ MeV}/c^2$ are slightly heavier than protons which have mass $938.3 \text{ MeV}/c^2$ [3]-(Sec 1.4). However, neutrons are unstable as free particles, and decay to protons according to reaction (1.8) [3]-(Sec1.4) with lifetime of 880.2 s via the weak forces. Also, protons and neutrons as they interact

via strong forces, each have the possibility to decay to neutrons and protons respectively within the nucleus under certain circumstances [3]-(Sec 1.4). Based on this fact, we realise that neither the neutron nor the proton is a fundamental particle, but in fact each consists of three quarks.

$$n \rightarrow p + e^{-} + \bar{\nu}_e. \quad (1.8)$$

Therefore, the stability of a nucleus relies on the stability of the neutrons and protons. As the nucleus grows larger, the neutrons begin to outnumber the protons as discussed in (Sec 1.1). The stability of a nucleus is a function of N as shown in the *Segrè* chart [3]-(Sec 2.4) **Figure 1.2**, which shows the stable nuclei through a plot of Z vs N . Thus, as the nucleus becomes bigger, the so-called line of stability moves further away from $Z=N$. This chart shows that the end products of fusion of light nuclei like deuterium are usually light and stable nuclei, whereas the end products of fission are heavy and unstable nuclei.

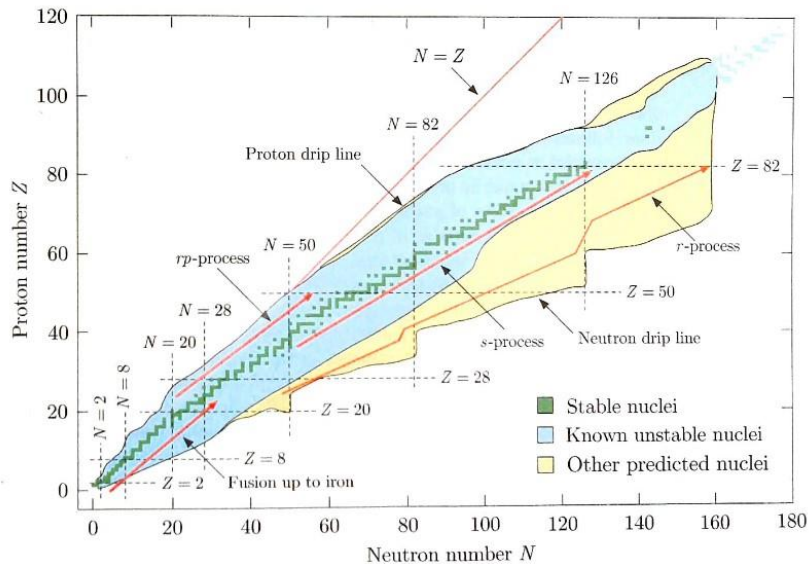
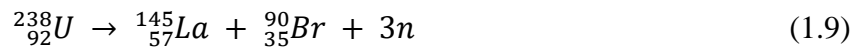


Figure 1.2. Segrè chart for stable and unstable nuclei [3]-(2.4).

Segrè chart, shows that, the stable nuclei lie in a very narrow band, and other nuclei are unstable, decaying in one of three ways [3]-(Sec 2.4), while emitting accompanied radiation. The following sections describe the three decay types.

1.2.1 Spontaneous fission and/or ejecting alpha particles (α)

Nuclei with $A > 100$ may undergo spontaneous fission [3]-(Sec 2.7), where the parent nucleus breaks into two nuclei without external action. as in the case of uranium:



For the case illustrated in reaction (1.9), the daughter nuclei have almost the same proportions of Z/N as uranium, thus they fall away from the stable nuclei band, and will continue decaying until stability is reached.

A heavy nucleus may also undergo alpha decay, where it ejects an alpha particle (α) which is the stable nucleus of helium, as in the case of uranium decaying to thorium:



1.2.2 Beta (β) decay

This decay occurs when a neutron, or a proton decays to a proton or neutron respectively.

A free neutron decays spontaneously to a proton according to reaction (1.8) because the neutron is heavier than the proton. This process also occurs within an unstable nucleus but with different lifetimes that vary from milliseconds to 10^{16}

years [3]-(Sec 2.6). In the case of neutron decay releasing an electron and an anti-neutrino, the value of A stays the same while Z increases as per the following examples [3]-(Sec 2.6).



Although it is not possible for a free proton to decay to a neutron and positron, positron emission is possible within an unstable nucleus because of the binding energy, according to reaction (1.14). In this case the value of Z will decrease, as in the case of ${}^{15}\text{O}$.



Electron capture is a process similar to β^{+} decay, where a nucleus captures one of the electrons surrounding it and changes a proton to a neutron as per (1.16), i.e.



1.2.3 Gamma decay (γ)

This type of decay usually occurs after the previously mentioned types of decay, or after a nuclear reaction, where the final nucleus is left in an excited state [5]-(Sec 6.5). If this excited state is below the threshold for spontaneous fission or alpha radiation, the components of the nucleus rearrange, allowing it to de-excite

by emitting one or more high-energy photons without changing the nucleus. Since this photon is released from within a nucleus, the dimensions of the source are on the scale of (10^{-15} m). Therefore, according to equation (1.18); the released energy is a few MeV if we take into consideration ($hc=1240$ MeV. fm) [5]-(Sec 6.5).

$$E = hc/\lambda \quad (1.18)$$

1.3 Nuclear Fission

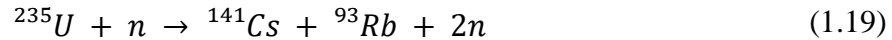
The discovery of neutrons by *Chadwick* in 1932 [5]-(Ch13) gave a new tool to explore the nature of matter and its nuclei, by exposing various nuclei to neutrons.

In 1938 *Enrico Fermi* won the Nobel prize for discovering that many nuclei decay by β^- emission following neutron capture, which means an increase in the atomic number. Consequently, this technique was used to produce transuranic² elements, which led to a series of subsequent experiments and discoveries.

Irradiating uranium with neutrons revealed that β^- was released. Soon after, studies showed that barium was produced as well, and the energy released was of the order of 100 MeV. That led *Meitner* and *Frisch* in 1939 to propose that the uranium nuclei became highly unstable and split almost in half after neutron capture [5]-(Ch 13). This process was later called fission which occurs as a result of disturbing the balance between Coulomb and the strong force. There is a similarity between induced and spontaneous fission, in term of the daughter

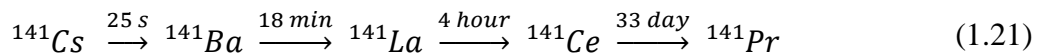
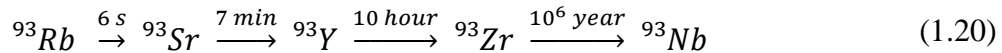
² Transuranic elements (also known as transuranium elements). Appendix A.

nuclear as illustrated in reaction (1.19) [5]-(Sec13.2), the difference is that in the induced fission, the probability of occurrence is much higher.



Therefore, fission can be applied to any nucleus that has been targeted by neutrons with enough excitation energy. However, to gain energy it is practical to use a heavy nucleus like uranium.

Reaction (1.19) above shows that uranium initially split into cesium and rubidium, which are highly radioactive, and subsequently decay emitting β^- [5]-(Sec 13.2) according to reactions (1.20) and (1.21):



The above discovery was the start of understanding nuclear fission; However, controlled fission required a better grasp of the relationship between neutron energy and the cross section of fissionable material.

1.3.1 Neutron interaction with matter.

Neutrons decay to protons within 15 minutes, thus free neutrons do not exist naturally but may be produced in a number of nuclear reactions (as in the interaction of beryllium with alpha and gamma radiation [5]-(Sec 12.1), which will be reviewed.

Since neutrons do not carry a charge, they can not be accelerated or decelerated, but it is possible to slow them down using material that allows the neutrons to collide to lose energy and slow down (moderator). Neutrons are classified according to their energies in **Table 1.2** [4]-(Sec 4-4).

Energy classification	Energy
Thermal	$E \approx 0.03 \text{ eV}$
Epithermal	$E = 0.03 \text{ eV} - 10 \text{ keV}$
Fast	$E > 100 \text{ keV}$

1.3.1.1 Neutron Sources

The beryllium reaction with alpha particles according to reaction (1.22) was behind the discovery of the neutron [5]-(Sec 12.1). This method is called the *Alpha-Beryllium Source*.



Usually, this reaction is possible when mixing beryllium with an alpha-emitting material like ${}^{226}\text{Ra}$, where the released neutrons' energy is distributed on a spectrum up to 13 MeV [5]-(Sec 12.1). The resulting neutrons from this reaction are not monoenergetic [5]-(Sec 12.1).

The other source of neutron production using beryllium is created by applying gamma radiation according to reaction (1.23). This method is called *Photoneutron*

Source. The advantage of this method is that we can have neutrons closer to monoenergetic [5]-(Sec 12.1).



Neutrons can also be produced in spontaneous fission and many nuclear reactions. However, the focus on beryllium comes from the important role it plays as a neutron multiplier, reflector etc... in nuclear fission reactors and as plasma facing material in nuclear fusion reactors [6]. Thus, it is important to understand the interaction of neutrons with matter through the definition of the cross section³.

1.3.1.2 Neutron-Matter Cross-Section

The interaction of neutrons with matter depends on the target nuclei cross section and the intensity of the neutron beam. The intensity is defined as the energy passing through unit area, per unit time.

Assuming a monoenergetic and monodirectional beam of n [neutrons/cm³] fired on a thin sample of density N [atoms/volume], has an area a and a thickness dx as shown in **Figure 1.3**. Since all n neutrons travel at the same speed v in the same direction, the intensity is then calculated according to equation (1.24) [4]-(Sec 2-1). the reaction rate in the entire sample is proportional to the target cross section, density, volume, and neutron beam intensity I , and is calculated according to equation (1.25).

³ Cross section is also defined as the probability of a certain nuclear reaction occurring.

The intensity according to the definition is:

$$I = n\left[\frac{1}{\text{cm}^3}\right]v\left[\frac{\text{m}}{\text{s}}\right] = nv\left[\frac{1}{\text{cm}^2 \cdot \text{s}}\right] \quad (1.24)$$

Where n is the number of neutrons per unit volume in the beam fired toward the target.

$$\begin{aligned} & \text{reaction rate in the target} \left[\frac{\text{reaction}}{\text{s}}\right] \\ &= (\sigma[\text{cm}^2])(I\left[\frac{1}{\text{cm}^2 \cdot \text{s}}\right])(N\left[\frac{1}{\text{cm}^3}\right])(a[\text{cm}^2])(dx[\text{cm}]) \end{aligned} \quad (1.25)$$

Therefore, if the value of the reaction rate was experimentally determined, the value of the cross section would be determined. assuming the intensity of the neutron beam stays monoenergetic and monodirectional over the entire target.

Usually, the cross section is measured with the unit of barn ($1 \text{ barn} = 10^{-24} \text{ cm}^2$), this unit is comparable to the small dimensions of nuclei and subatomic particles.

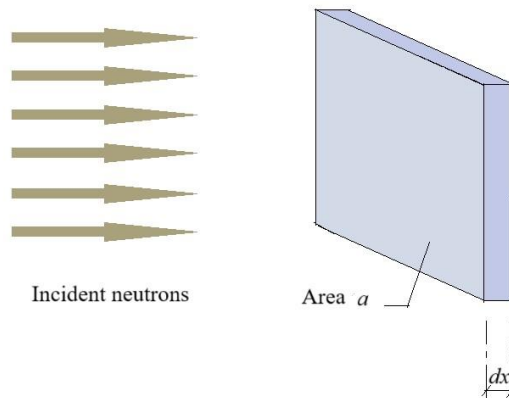


Figure 1.3. Neutron incident on a target.

The previous assumption regarding the neutron beam staying monoenergetic and monodirectional over the entire sample is not accurate, because neutrons interact with the nuclei of the target in a different way, like elastic scattering, inelastic scattering, radiative capture, and fission. Thus, the neutrons in the beam will be scattered as they pass through the sample. Hence, to reduce the error, it is better to reduce the sample thickness and density as we will see later, during the verification and benchmarking process.

1.3.2 Controlled Fission Reaction.

In fission reactions like reaction (1.19), neutrons are emitted, most of these neutrons appear instantaneously within about 10^{-17} of a second of the fission process, those are the prompt neutrons [4]-(Sec 3-4).

Less than 1% of the fission neutrons appear long after the end of the fission event, they are called the delayed neutrons [4]-(Sec 3-4). Delayed neutrons are the product of neutron emission by a radioactive decay of some fission product. Although delayed neutrons play an important role in reactor operation, they will not be discussed in this research.

The average number of prompt neutrons for ^{235}U fission is 2.44 [4]-(Sec 3-3). They are emitted with a continuous distribution of energy as shown in **Figure 1.4** [4]-(Sec 3-4).

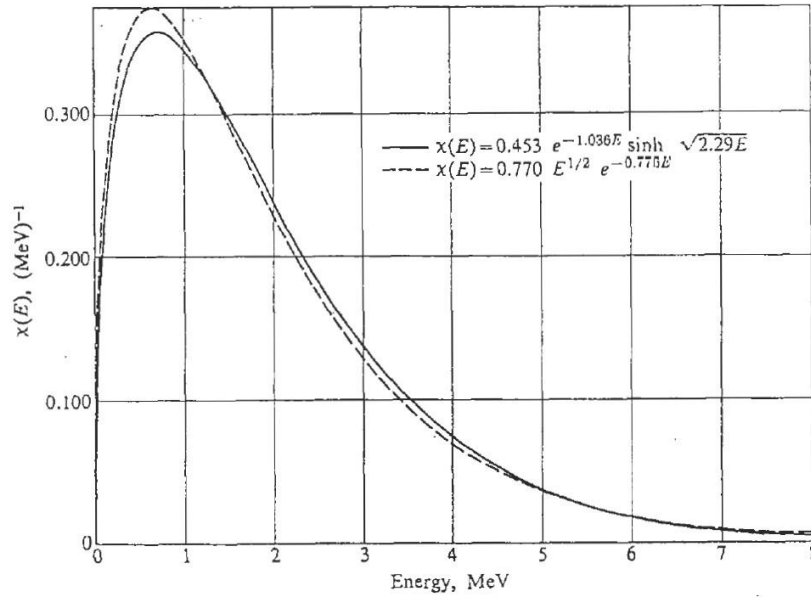


Figure 1.4. Distribution of prompt neutrons energy after ^{235}U fission reaction [4]- (Sec 3-4).

This continuous distribution of energy is described by a $\chi(E)$, which is called the prompt neutron spectrum, has been derived based on experimental data over the years, the most recent is given in equation (1.26). Experimental data show that $\chi(E)$ is independent of the energy of the neutron inducing the fission [4]- (Sec 3-4).

$$\chi(E) = 0.453e^{-1.036E} \sinh \sqrt{2.29E}, E \text{ in MeV} \quad (1.26)$$

The mean energy is about 2 MeV, and since there are about 2.44 prompt neutrons for ^{235}U , the average would be about 5 MeV. Knowing that the cross section of ^{235}U is higher when the incident neutron energy ≤ 1 eV, as shown in **Figure 1.5**, it is necessary to reduce the energy of at least one of these neutrons to allow for the next fission reaction, which is a process called moderation. After the moderation, if the number of neutrons that are within the range of energy to induce fission is

more than the number of neutrons of the previous fission, the fission rate⁴ would increase and become out of control.

Thus, it is important to control the number of neutrons and their energies to keep the number of fissions occurring per unit time constant.

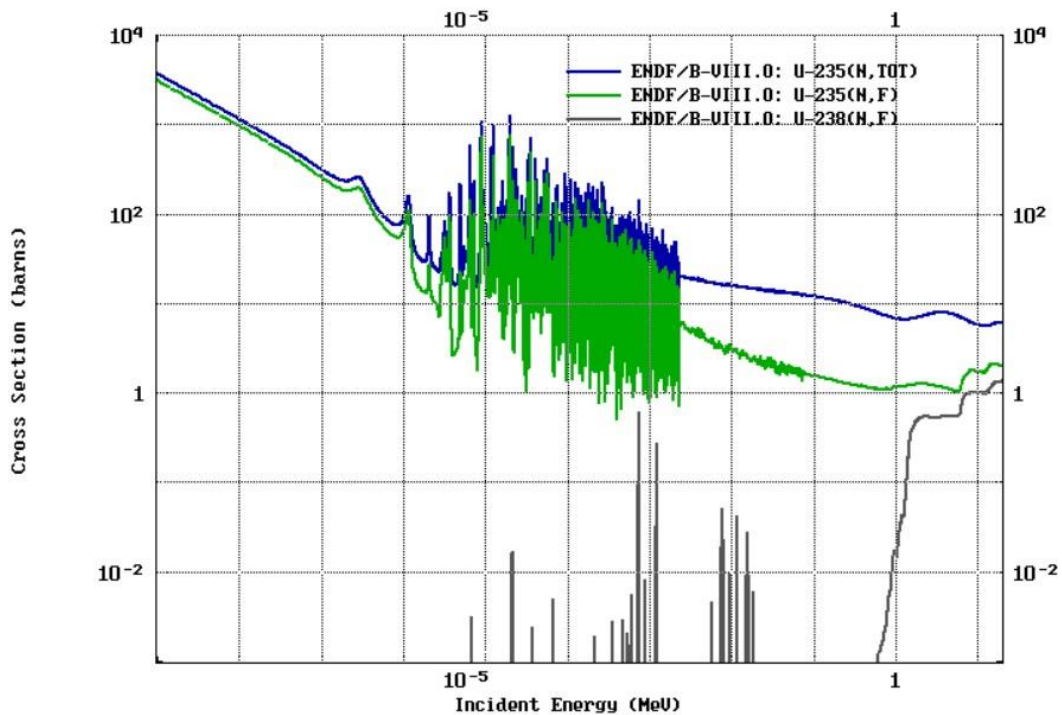


Figure 1.5. Cross section for neutron-induced fission of ^{235}U and ^{238}U [7].

1.3.2.1 Multiplication Factor and Criticality Requirements

In the previous paragraph we saw that both the number of neutrons produced and their energy play an important role in keeping the nuclear fission reaction steady. The ratio of the number of neutrons in one generation to the number of neutrons

⁴ Fission rate depends on the product σv , where σ is the fission cross section and v is the neutron velocity.

in the preceding generation is called the *multiplication factor* k , which plays an important role in reactor design [4]-(Sec 4-1). It can take the following values:

- $k > 1$: the number of fissions increasing with each succeeding generation; the reactor is supercritical.
- $k = 1$: the number of fissions in each succeeding generation is constant; the reactor is critical.
- $k < 1$: the number of fissions in each succeeding generation is decreasing; the reactor is subcritical.

To be able to generate steady power from a fission reaction the multiplication factor must equal unity. Maintaining a critical reaction process requires a balance between production and disappearance of neutrons at a specific energy [4]-(Sec 4-1). Without listing the detailed mathematical equations used to accomplish these conditions, a brief description of the main reactor components and their roles is included below:

1.3.2.2 Type of Fuel

Fuel material is described as fertile or fissile. Fissile material is a term used to describe isotopes most likely to undergo a fission process after absorbing thermal energy neutrons [4]-(Sec 3-1) like ^{235}U , ^{233}U and ^{239}Pu . Whereas fertile material refers to isotopes, that are not fissile but can converted to fissile materials. ^{238}U which only undergoes a fission reaction with high energy neutrons is a fertile isotope.

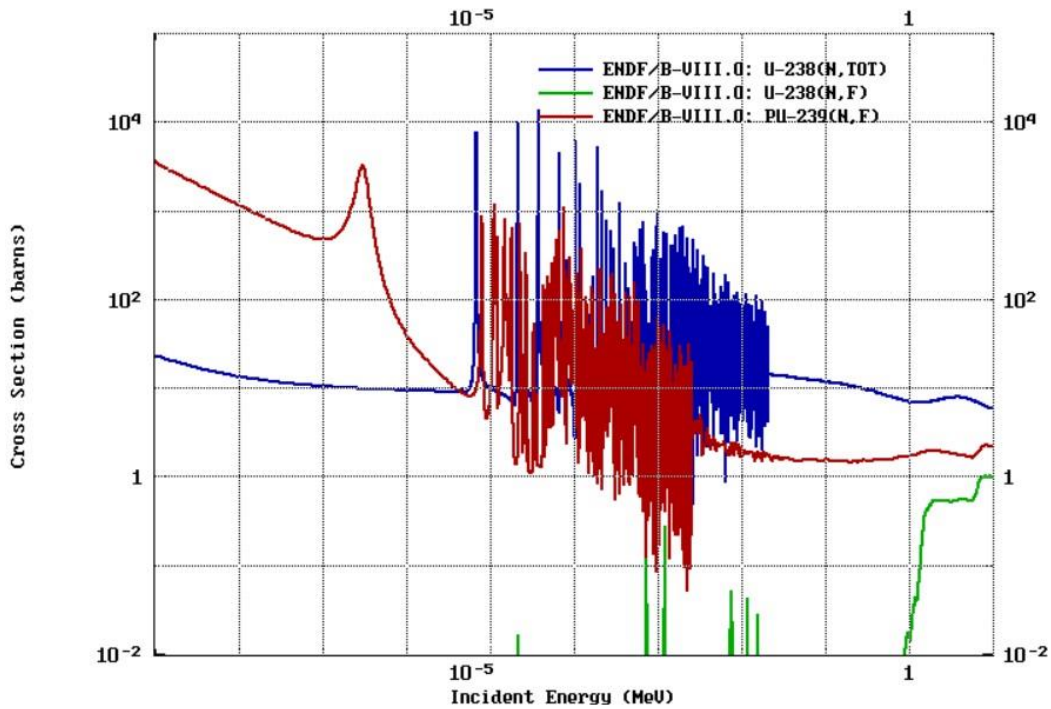


Figure 1.7. Total and fission cross section of ^{238}U and fission cross section of ^{239}Pu [7].

Thus, each type of nuclear fission fuel has a different neutron cross section and releases a different number of emitted neutrons based on the chosen combination of fissile and fertile materials, as well as fuel density.

1.3.2.3 Moderator

The average energy of the prompt neutron is 5 MeV. This energy can be reduced by placing a specific material (the moderator) whose atoms collide with high energy neutrons and slow them down without absorbing them. Thus, the moderator should satisfy the following [5]-(Sec 13.6):

- Neutrons lose on average more energy in elastic collisions with light nuclei than with heavy nuclei. Therefore, a light element such as carbon is desirable to slow down the neutrons efficiently.
- The moderator should have a very small neutron capture cross section.

There are several different materials used as moderator. The choice relies on the size of the reactor, intended energy output, and fuel type. The most common type of moderators are graphite, light water, and heavy water.

1.3.2.4 Control rods

While the moderator adjusts the neutron energy, the role of the control rods is to keep the number of neutrons around the fuel at a specific value [4]-(Ch 14) There are several elements for the purpose of control, like boron and cadmium, hafnium and boron [4]-(Ch 14).

1.3.2.5 Coolant

The coolant removes the heat from the fuel and uses it to boil water to produce pressurized steam, Then, the steam spins turbine blades that drive magnetic generators to produce electricity [5]-(Sec 13.6). Coolants can be liquids (like water, molten salt, or liquid metal), and gases (like CO₂ or helium). The choice relies on the size of the reactor, fuel type and intended energy output.

1.3.3 Nuclear Fission Reactor Types

Classification of nuclear fission reactors is diverse; because the classification relies on multiple factors like neutron energy, fuel type, coolant, size, and final

purpose. Following are descriptions of CANDU (currently the primary source of tritium globally), and MSR (the focus of this study).

1.3.3.1 Canadian Deuterium Uranium (CANDU)

This Canadian reactor uses natural uranium, and a deuterium oxide (heavy water) moderator. The main advantage of this reactor is the use of natural uranium, which reflects on the unique design and size as represented in the schematic seen in figure [5]-(Sec 13.6).

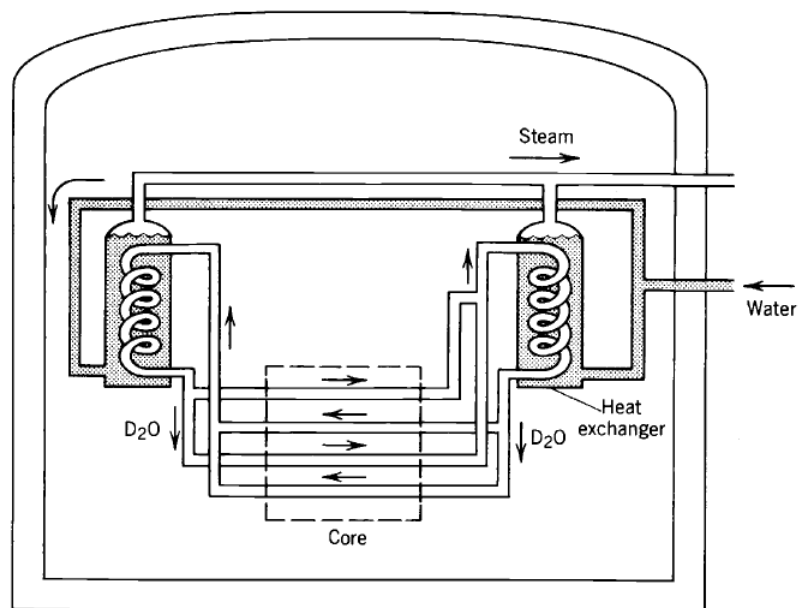


Figure 1.8. Schematic diagram CANDU [5]-(Sec 13.6)

In CANDU, the fuel is placed horizontally in a long pressure tube traversing the core which is contained within a large cylindrical vessel called the *calandria*. The moderator fills the whole calandria, while the coolant passes through the pressure tubes to transfer the heat generated in the fuel. Since the coolant is kept under

high pressure, CANDU is classified as a pressurized water reactor (PWR). Most importantly, the use of heavy water as a moderator allows CANDU to produce larger quantities of tritium than most nuclear fission reactors as will be explained in (Chapter 2 – Sec 2.1).

1.3.3.2 Molten Salt Reactors - MSRs

Molten Salt Reactors are non-conventional nuclear power reactors. They use low pressure molten fluoride (or chloride) salts as a coolant and/or the fuel is a molten salt mixture.

All molten salt reactor technology originates from the Molten Salt Reactor Experiment (MSRE) developed by Oak Ridge National Laboratory in Tennessee. So far, it is the only MSR that ever operated, and it was operating from 1965 to 1969.

The MSR – shown in **Figure 1.9** – (which will be revisited in more depth in Chapter 3 as it is the core of this study) - demonstrates how as the chain reaction occurs, the temperature of the fuel increases causing the fuel salt mixture to expand and rise, As the fuel salt mixture expands, its density decreases.

The increase in temperature and decrease in density will slow the chain reaction for the following reasons:

- If a reactor is critical at a specific temperature, increasing the temperature will make neutrons appear faster (more energetic than its actual energy) to the fissile isotopes. Thus, according to **Figure 1.5****Figure 1.6****Figure 1.7**

$$V_C = \frac{Z_a Z_b e^2}{4\pi\epsilon_0(R_a + R_b)} \quad (1.29)$$

Where Z_a and Z_b are the atomic number of nucleus a and nucleus b respectively, R_a and R_b are the radius of the nucleus, which can be approximated by equation (1.2). ϵ_0 is the permittivity of vacuum, and e is the charge of electron.

As Z_a and/or Z_b increase, the Coulomb potential barrier increases, therefore fusion is more probable as Z decreases.

Using equation (1.2), and substituting the values⁵ of e and ϵ_0 , it is possible to rewrite equation (1.29) for simplification as:

$$V_C = 1.19 \frac{Z_a Z_b}{A_a^{1/3} + A_b^{1/3}} \text{ [MeV]} \quad (1.30)$$

Thus, for small nuclei like deuterium and tritium (isotopes of hydrogen), the energy required to overcome the Coulomb potential barrier is about 0.4 MeV. This energy is not difficult to achieve using a particle accelerator⁶. But it is impossible to make an accelerator to produce net fusion energy, because the elastic scattering of charged particles will cause the energy to dissipate.

This issue is explained in the following example given by *Alexander Piel* [9]-(Sec 1.5.1). As shown in **Figure 1.10** [9]-(Sec 1.5.1) when shooting a 1 ampere beam of tritium ions (which is $\frac{1 \text{ Amp}}{e} = 6.3 \times 10^{18}$ ions per second) into a 1 cm^3 target containing (5.4×10^{19} deuterium atoms), the probability of hitting one of the

⁵ Refer to Appendix C for list of constants.

⁶ Particle accelerators are devices that produce and accelerate beams of charged particles, such as electrons, protons, and ions [30]

deuterium nuclei is the ratio of the area blocked by deuterium nuclei to the area of one of the cube faces. If one deuterium area is calculated using equation (1.2) and multiplied by the total number of deuterium nuclei, then the result divided on 1 cm^2 , the probability can be shown to be:

$$\begin{aligned} R_{deuterium} &= 1.21A^{1/3} = 1.21(2^{1/3}) = 1.52 \text{ fm} \\ &= 1.52 \times 10^{-13} \text{ cm} \end{aligned} \tag{1.31}$$

$$\begin{aligned} a_{deuterium} &= \pi(1.52 \times 10^{-13})^2 \times 5.4 \times 10^{19} \\ &= 3.92 \times 10^{-6} \text{ cm}^2 \end{aligned} \tag{1.32}$$

$$p = \frac{a_{deuterium} [\text{cm}^2]}{1 [\text{cm}^2]} = 3.92 \times 10^{-6} \tag{1.33}$$

If each successful fusion reaction releases 17 MeV energy (see Sec 1.4.1), then the total fusion power per cubic meter is:

$$\begin{aligned} \text{Total fusion power} &= p \times 6.3 \times 10^{18} \left[\frac{\text{tritium ions}}{\text{second}} \right] \times 17 [\text{MeV}] \\ &= 4.2 \times 10^{20} \left[\frac{\text{eV}}{\text{second}} \right] \times 1.6 \times 10^{-19} [\text{J}] \\ &= 67 \left[\frac{\text{W}}{\text{cm}^3} \right] \end{aligned} \tag{1.34}$$

If each tritium ion has 100 keV, then the total spent energy is 100 kW, while the output is much smaller.

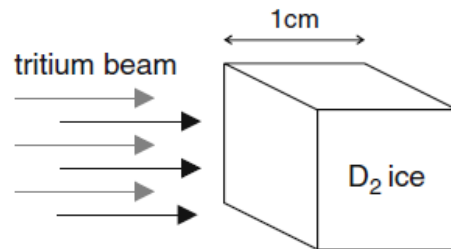


Figure 1.10. Tritium ions beam hitting a deuterium ice-cube [9]-(Sec 1.5.1).

1.4.1 Nuclear Fusion Requirements

The energy of the sun (heat or light energy) comes from the nuclear fusion process continuously occurring in its core. Where the high temperature (15.7 million K) provides nuclei with enough energy to overcome their mutual electrical repulsion, and massive gravity produces high pressure, making it possible to fuse protons and release helium as shown in **Figure 1.11** [10].

To create fusion on earth, (aside from the need to create some kind of confinement), a light element (hydrogen) gas needs to be pressurised and heated to about 150 million K, (about 10 times the temperature in the Sun's core), to compensate for energy lost in scattering from the lack of conditions produced by the massive gravity on the sun.

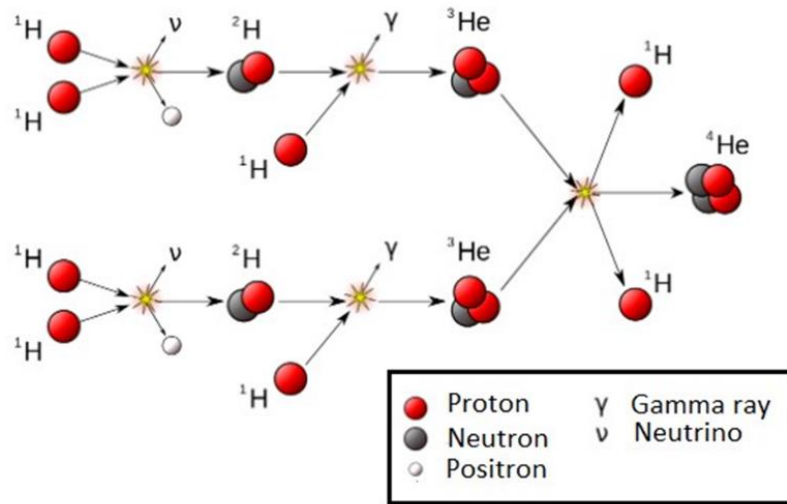
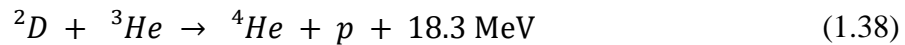
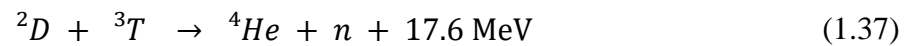
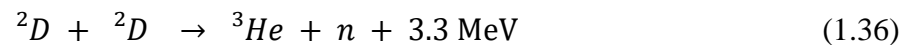
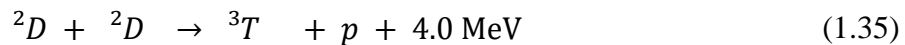


Figure 1.11. Fusion chain reaction on the Sun [10].

To achieve fusion on earth, only limited types of nuclear fusion reaction have a chance for success [9]-(Sec 1.5). These reactions are (1.35), (1.36), (1.37) and (1.38) releasing energy in the form of kinetic energy of the products:



Each of the above fusion reactions must achieve a specific centre-of-mass kinetic energy to overcome Coulomb repulsion. **Figure 1.12** illustrates the change of the cross section as a function of centre-of-mass kinetic energy [9]-(Sec 1.5). It shows that for energies between 10 and 100 keV, the D-T⁷ reaction has the highest cross

⁷ Tritium is a hydrogen isotope that can be written as (³H, or T).

section. Thus, the D-T reaction has been selected for most controlled fusion reaction experiments and research.

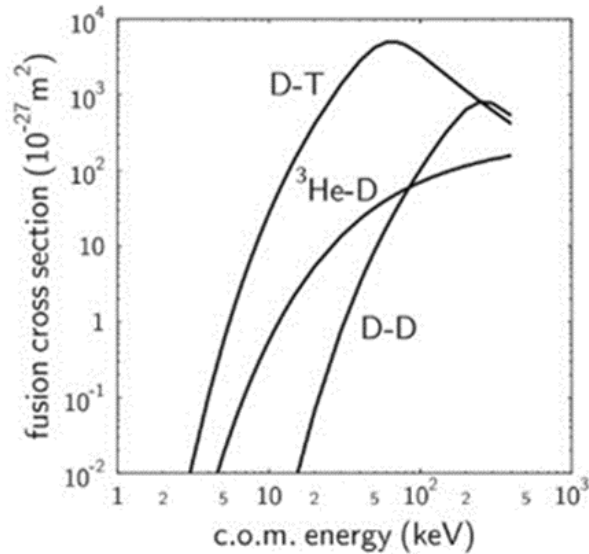


Figure 1.12. The cross-section of D-T, D- ^3He and D-D fusion reactions [9]-(Sec 1.5).

Previously, it was illustrated that accelerating particles will not lead to net fusion energy. Therefore, we need three conditions: a) high temperature to increase particle energy, b) confinement in a small place to bring nuclei close to each other, and c) enough time in confinement to increase the chances of collision.

If the temperature is increased enough, the confined fuel mixture (D-T) becomes a hot cloud of positive ions and negative electrons while remaining neutral overall. This state is called *plasma*⁸. Without going into the details of the dynamics that control plasma behavior, some of the factors that have an effect when designing nuclear fusion reactors will be visited.

⁸ Plasma is a state of a superheated matter, so hot that the electrons break away from the atoms forming an ionized gas while the matter remains neutral overall.

1.4.1.1 Debye Shielding

In a plasma, any charged particle attracts other particles with opposite charge and repels those with the same charge, causing each charged particle to be surrounded by a net cloud of opposite charges shielding its electrostatic potential field. This is *Debye shielding*.

To demonstrate the effect of Debye shielding, consider a positive test charge Q placed in a large, neutral plasma of protons and electrons (hydrogen plasma), the original density of protons (n_p) equals the original density of electrons (n_e) because of overall charge neutrality ($n_p = n_e = n$) [9]-(Sec 2.2.1).

The electrostatic potential $\phi(r)$ outside the test particle should satisfy Poisson's equation according to equation 1.39).

$$\nabla^2 \phi(r) = -\left(\frac{(n_p(r) - n_e(r)) + Q\delta(r)}{\epsilon_0}\right) \quad 1.39$$

Where, $\delta(r)$ is the delta⁹ function, and r is the radial distance.

If the plasma was cold with no thermal motion, then there would be a fixed number of electrons carrying the opposite charge of the test particle, and the field would be perfectly shielded. But the plasma is very hot, thus, the speed distribution of its electrons and ions follows *Maxwell-Boltzmann* distribution, and the mean kinetic energy of the electrons and ions is $\frac{3}{2}k_B T$ [11]-(Sec 5.2.2), where, k_B is the Boltzmann constant and T is the plasma temperature in Kelvin. The

⁹ See Appendix C.

expected edge of the cloud occurs where the potential energy is approximately equal to the mean thermal kinetic energy $e\phi(r) = \frac{3}{2}k_B T$.

Since the plasma was originally neutral, the insertion of the test particle will alter the density of the protons and electrons according to their distance from the test particle. Thus, a proton at distance r from the test particle has an electrostatic potential energy $e\phi(r)$, and its density altered by the Boltzmann factor¹⁰ [11]- (Sec 4.6) according to equation (1.40), and, similarly, the density for the electron according to equation (1.41).

$$n_p(r) = n \exp(-e\phi/k_B T) \approx n(1 - e\phi/k_B T) \quad (1.40)$$

$$n_e(r) = n \exp(-e\phi/k_B T) \approx n(1 - e\phi/k_B T) \quad (1.41)$$

Substitute (1.40) and (1.41) in equation 1.39);

$$\nabla^2 \phi = \frac{\partial^2 \phi}{\partial r^2} + \frac{2}{r} \frac{\partial \phi}{\partial r} = \frac{2e^2 n}{\epsilon_0 k_B T} \phi - \frac{Q}{\epsilon_0} \delta(r) \quad (1.42)$$

The spherically symmetric solution to this equation is:

$$\phi(r) = \frac{Q}{4\pi\epsilon_0 r} \exp\left(\frac{-\sqrt{2}r}{\lambda_D}\right) \quad (1.43)$$

The parameter λ_D , is identified as:

$$\begin{aligned} \frac{1}{\lambda_D^2} &= \left(\frac{e^2 n}{\epsilon_0 k_B T}\right)_{\text{From the electron}} + \left(\frac{e^2 n}{\epsilon_0 k_B T}\right)_{\text{From the proton}} \\ &\rightarrow \frac{1}{\lambda_D^2} = \frac{1}{\lambda_{D-e}^2} + \frac{1}{\lambda_{D-p}^2} \end{aligned} \quad (1.44)$$

¹⁰ The term $\exp(-\text{Energy}/k_B T)$ is known as the Boltzmann factor. Refer to Appendix C

Now, if the test particle was just an ion, that means the above solution can be applied to any charged particle within the plasma, where each proton is shielded by a spherical cloud of electrons with a radius λ_{D-e} , which is bigger than λ_D . Thus, to guarantee the fast decrease of the potential before moving into the neighbouring ion cloud, Debye length is approximated by $\lambda_D = \lambda_{D-e} = \lambda_{D-p}$ according to equation (1.45). Also, for $r > \lambda_D$, the electric potential around the test charge will decay exponentially with $\exp(-1)$ factor.

$$\lambda_D = \left(\frac{\epsilon_0 k_B T}{e^2 n} \right)^{1/2} \quad (1.45)$$

Thus, each proton carries a negatively charged Debye shielding cloud of size λ_D as it moves in the plasma, while the electrons carry a positively charged cloud. Also, each charged particle of the contributors to the clouds around other electrons and protons have their own cloud.

Since, the temperature of the plasma should be high, the density has an immediate effect on λ_D . Debye length represents the distance within which separate charges can be present inside the space of an overall neutral plasma, due to the presence of potential and thermal energy. Thus, the physical dimensions of the system should be greater than Debye length.

1.4.1.2 Fusion Reaction Rate

As discussed in **Sec 1.3.2**, the fission cross section of ^{235}U relies on neutron energy/velocity, also seen in **Figure 1.5** which shows that $\sigma \propto \frac{1}{v}$ outside the resonance region, so $\sigma v = \text{constant}$ [5]-(Sec 12.4).

This is not the case for fusion, because the distribution of particle speeds at a specific plasma temperature, are described by Maxwell-Boltzmann distribution, Thus, the fraction of particles with speeds between v and $v+dv$ can be defined as $f(v)dv$ according to equation 1.46) [11]-(Sec 5.2).

$$f(v)dv = \left(\frac{2}{\pi}\right)^{1/2} \left(\frac{m}{k_B T}\right)^{3/2} \exp\left(\frac{-mv^2}{2k_B T}\right) v^2 dv \quad (1.46)$$

Where m is the reduced mass of the particles in the plasma. Therefore, in a fully ionized plasma of deuterium and tritium, with density n_D , and n_T respectively, at a temperature T , the fusion reaction rate per unit volume can be written according to equation (1.47) [3]-(Sec 9.2.2), and assuming we have 50% deuterium and 50% tritium with total particle density, $n = n_D + n_T$.

$$R_{DT} = n_D n_T \langle \sigma_{DT} v \rangle = \frac{1}{4} n^2 \langle \sigma_{DT} v \rangle \quad (1.47)$$

Where, σ_{DT} is D-T fusion cross section at a temperature T , and the brackets denote an average according to 1.48) [3]-(Sec 9.2.2).

$$\langle \sigma_{DT} v \rangle = \int_0^{\infty} \sigma_{DT} v f(v) dv \quad (1.48)$$

1.4.1.3 Lawson Criterion

The energy content per unit volume of a hot isothermal deuterium-tritium plasma with temperature T and plasma density n , is.

$$E_{th} = \frac{3}{2} k_B (n_e T_e + n_D T_D + n_T T_T) = 3nk_B T \quad (1.49)$$

Where n_e is the density of electrons in a quasi-neutral¹¹ D-T plasma, therefore $n_e=n$. T_e , T_D and T_T , are the temperature of the electrons, deuterium ions and tritium ions respectively, and should equal T , the temperature of the plasma, because all charged particle in the plasma are in thermal equilibrium.

Considering equation (1.47), the expected total energy is as represented in equation (1.50) assuming 100% efficiency.

$$E_t = \frac{1}{4}n^2\langle\sigma_{DT}v\rangle Q\tau \quad (1.50)$$

Where Q is the energy released per reaction (for D-T the total is 17.6 MeV, only the 14 MeV carried by the neutrons is useable for energy generation) and τ is the confinement time. However, in a confined plasma, there will be many types of energy loss, the most dominant being the *Bremsstrahlung* loss (E_{br}). In the *Bremsstrahlung* loss, coulomb scattering produces an acceleration affecting the lightest particles (electrons), which consequently lose energy, but because the ions and the electrons are in thermal equilibrium, the ions will also lose energy [5]- (Sec 14.4). Also, for every passing second the plasma loses heat.

Assuming the energy provided to heat the plasma is E_{th} , and the plasma was confined for a time τ , the generated fusion energy E_t , while ignoring the efficiency factor, the reactor shows a positive net energy if $E_t > E_{th}$. Thus, the reactor needs to satisfy the following [5]-(Sec 14.4).

¹¹ The plasma is a quasi-neutral, because of the charge neutrality. For hydrogen plasma the number of electrons is equal to the number of ions.

$$\frac{1}{4}n^2\langle\sigma_{DT}v\rangle Q\tau > 3nk_B T \quad (1.51)$$

$$n\tau > \frac{12k_B T}{\langle\sigma_{DT}v\rangle Q} \quad (1.52)$$

Since $\langle\sigma_{DT}v\rangle$ is a function of the temperature T according to equations 1.46) and 1.48), where v can reach a maximum according to equation (1.53) [11]-(Sec 5.2.2), $T/\langle\sigma v\rangle$ is a function of T and has a minimum. Thus, it is more accurate to include the temperature in Lawson criterion, and rewrite it as a product of density n , temperature T and confinement time τ , according to equation (1.54).

$$v_{max} = \sqrt{\frac{2k_B T}{m}}, \quad (1.53)$$

m is the reduced mass of (deterium – tritium)

$$nT\tau > \frac{12k_B T^2}{\langle\sigma_{DT}v\rangle Q} \quad (1.54)$$

The Lawson criterion informs guidelines allowing reactor designers to set the proper operating temperature, plasma density and confinement time. **Figure 1.13** below illustrates Lawson's criterion for steady state operation and for different efficiency values [9]-(Sec 4.4.2.3).

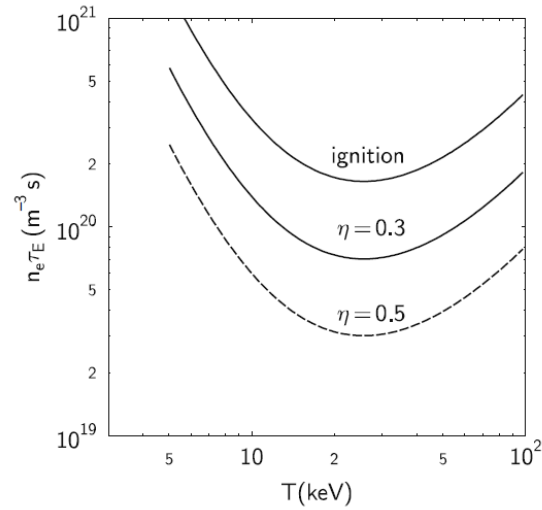


Figure 1.13. Lawson's criterion [9]-(Sec 4.4.2.3).

1.4.2 Methods of Nuclear Fusion Confinement

As previously discussed, to achieve a nuclear fusion reaction, two main conditions must be achieved - high temperature and confinement to minimise heat loss. These conditions are summarized in Lawson's criterion, which can be applied in two different circumstances: a) Magnetic confinement fusion, b) Inertial confinement fusion.

1.4.2.1 Magnetic Confinement Fusion

Magnetic confinement of hot plasma is the working principle used in the tokamak or stellarator. The focus in this method is to increase the confinement time close to $\tau = 1$ second [9]-(Sec 4.4.3). Thus, according to Lawson's criterion it is possible to reduce ion density.

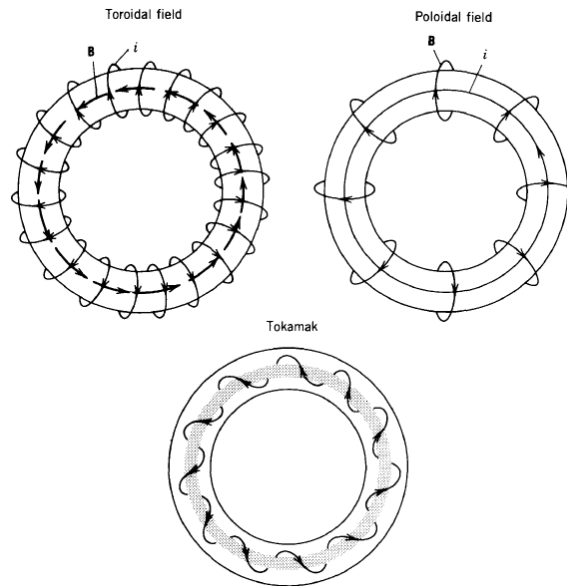


Figure 1.14. Principle of tokamak method of magnetic confinement [5].

The magnetic confinement is achieved by winding coils to produce a toroidal magnetic field that allows the plasma to spiral around it. A poloidal magnetic field is created to avoid the drift of the plasma toward the wall. Usually, the poloidal field is created using a set of external coils, or by passing a current through the plasma itself along the axis of the toroid. **Figure 1.14** shows a schematic of tokamak method of magnetic confinement.

Examples of Tokamak are ITER [2] in France and JET [12] in the UK.

1.4.2.2 Inertial Confinement Fusion

In Inertial Confinement Fusion (ICF), either intense laser radiation or X-rays are used on a spherical capsule to compress the D-T fuel inside the capsule to a density of about 1000-2000 times the density of D-T ice. [9]-(Sec 1.5.6).

Figure 1.15 is a schematic illustrating the principle of inertial fusion method.

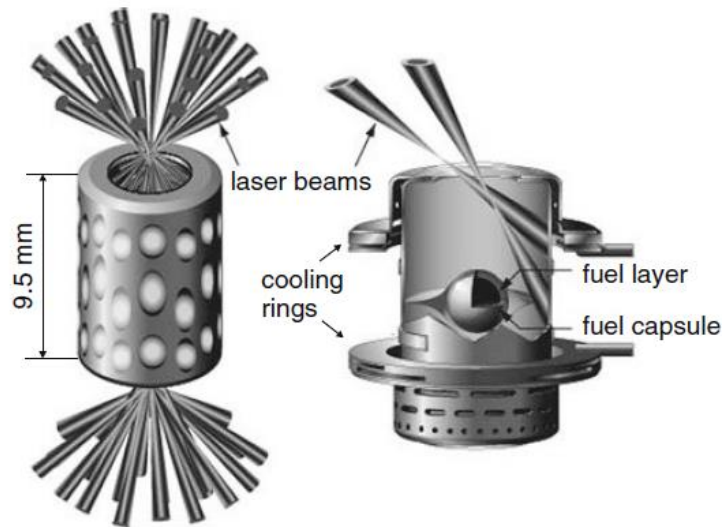


Figure 1.15. Inertial confinement fusion principale [9].

An example of ICF is the National Ignition Facility in California (NIF), USA, where a small spherical capsule containing deuterium and tritium is suspended in a cylindrical x-ray oven called a *Hohlraum* [13], as shown in **Figure 1.16**.

The fuel inside the capsule needs to be compressed for high density and heated to a high temperature. Thus, the outer surface of the capsule is heated by laser produced x-rays uniformly over its entire surface to cause uniform compression of the fuel to the center. To create this environment, laser beams enter the *Hohlraum* through holes in the end caps, heat the walls of the cylinder, which then radiate x-rays. Usually, the *Hohlraum* is made out of high Z material like Au [14].

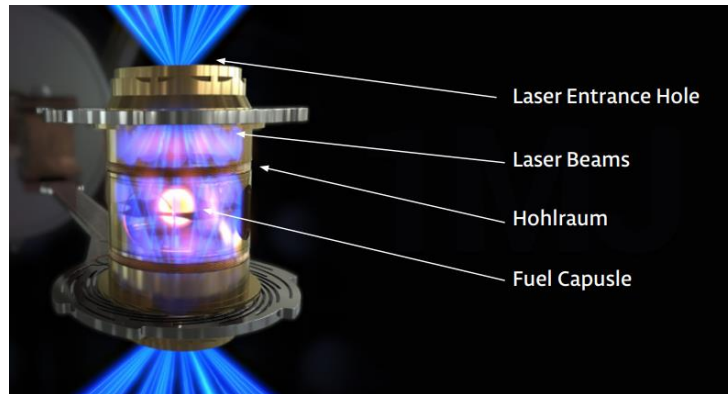


Figure 1.16. Schematic of a NIF ignition target. The fuel capsule is suspended inside gold or another high-Z [13].

Since the ICF method relies on high density of D-T fuel, then, according to Lawson's criterion the confinement time can be small. The ICF principle in summary relies on creating a tiny pellet containing high density deuterium and tritium heated and compressed directly or indirectly with an intense laser pulse.

1.4.3 Nuclear Fusion Fuel

Both magnetic confinement and inertial confinement face many challenges including but not limited to, the lack of available tritium. Providing tritium alone stands as one of the biggest challenges for future fusion power plants.

Tritium can be a by-product of fission reactors like CANDU, which generate about 130 g of tritium annually [1], which will make starting the ITER experiment possible. However, a future commercial fusion power plant is expected to consume 300g of tritium per day to produce 800 MW [2].

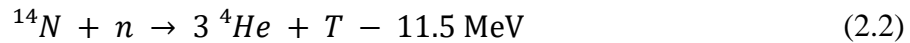
Chapter 2

Tritium Breeding

2.1 Tritium Issue

Tritium is a radioactive isotope of hydrogen with two neutrons. It decays emitting β^- radiation, ${}^3\text{He}$ and 18.59 keV, it has a half life of 12.3 years [15] [16].

It is very rare and most naturally available tritium is in the upper layer of the atmosphere originating from the interaction of cosmic rays with the gases there according to the following reactions [16].



The energies 4.3 MeV and 11.5 MeV are those required for reaction (2.1) and (2.2) to occur respectively, demonstrated in **Figure 2.1**. As discussed in the previous chapter, tritium is also a by-product of nuclear energy power plants like the CANDU.

CANDU reactors produce 130 g of tritium annually because of $D(n, \gamma)T$ reaction in the reactor core [1], as expressed in (2.3) [16].



However, about 300 g of tritium is needed daily to run an 800 MW fusion reactor.

This chapter discusses a possible method to generate tritium, and reviews some of

the ongoing research into tritium breeding, as well as highlighting the reason for choosing Molten Salt Reactor (MSR).

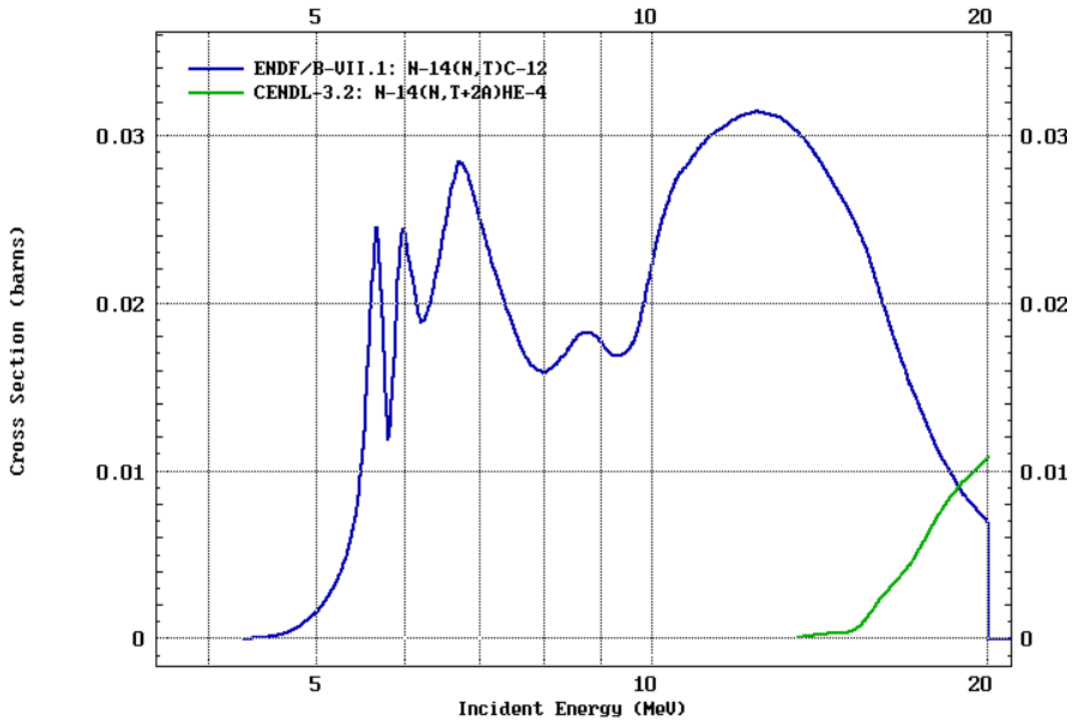
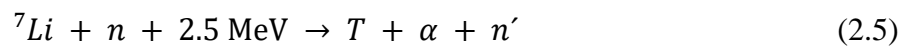


Figure 2.1. Energy threshold and cross section of ^{14}N interaction with neutron [7].

2.2 Role of Lithium in Tritium Production

It is possible to produce tritium using both stable isotopes of lithium ^7Li and ^6Li , because lithium interacts with neutrons according to the following combination of reactions [17].



Reaction (2.4), shows that the incident neutron does not require a high energy for the reaction, and releases 4.8 MeV carried by the reaction product. While reaction

(2.5) requires the incident neutron to have energy threshold of 2.5 MeV, therefore n' has less energy than the incident neutron. Thus, incident neutron energy has an important effect on tritium production.

The cross section of both isotopes of lithium interacting with neutrons to produce tritium, as a function of the incident neutron energy is presented in **Figure 2.2**.

Figure 2.2 also shows the ${}^6\text{Li}$ reaction has a high cross section when the neutron energy is less than 1 MeV, and confirms that for ${}^7\text{Li}$, the incident neutron should carry an energy of 2.5 MeV [17] before the cross section increases. Thus, the method used to investigate will differ depending on neutron energy and the lithium isotope used. Lithium is the lightest metal¹², the percentages of atomic abundances for naturally occurring lithium are ${}^7\text{Li}$ 92.5% and ${}^6\text{Li}$ 7.5%.

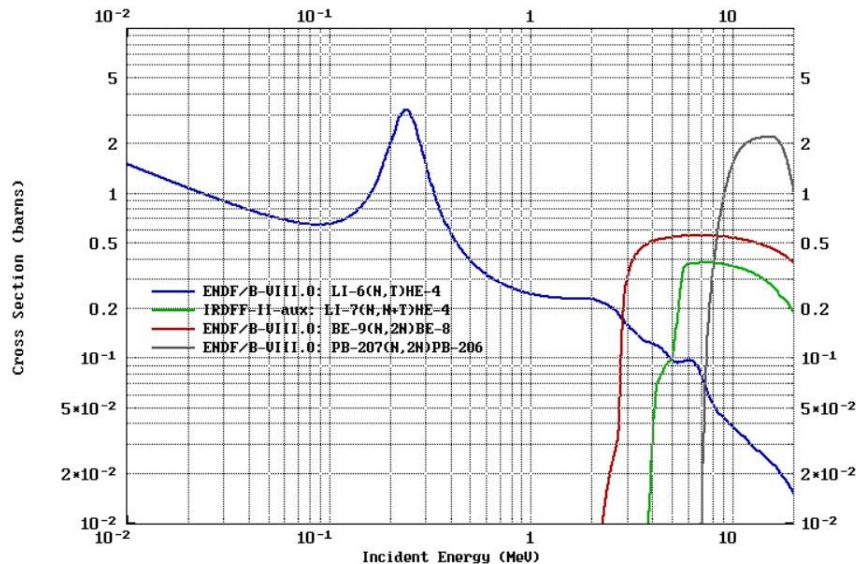


Figure 2.2. Cross section for neutron interaction as a function of energy for ${}^7\text{Li}$, ${}^6\text{Li}$, ${}^9\text{Be}$ and Pb [7].

¹² Lithium is the lightest Alkali metal. See Appendix A

2.3 Role of Beryllium in Tritium Production

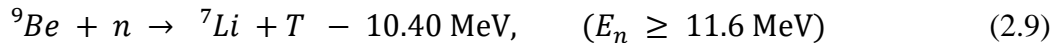
When beryllium interacts with a neutron of energy above 0.67 MeV it increases ${}^6\text{Li}$. This interaction can cause ${}^9\text{Be}$ to fission releasing unstable helium isotope ${}^6\text{He}$ according to reaction (2.6) [16].



The unstable ${}^6\text{He}$ has a half life $t_{1/2} = 0.807$ second and will decay to ${}^6\text{Li}$ according to reaction (2.7) [16]. However, increasing ${}^6\text{Li}$ does not necessary mean increasing tritium breeding, thus the effect of beryllium should be studied within a complete reactor environment.

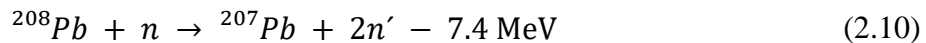


For neutron energy above 2.7 MeV, Beryllium acts as a neutron multiplier according to reaction (2.8), and produces tritium when the incident neutrons have energy above 10.40 MeV according to reaction (2.9) [16].



2.4 Role of Lead in Tritium Production

Lead, like beryllium, has a role as neutron multiplier when interacting with neutrons carrying energy above 7.4 MeV according to reaction (2.10) [16].



Both beryllium and lead play an indirect role in breeding tritium, thus, the choice of using beryllium or lead depends on the design requirements.

2.5 Concurrent Tritium Breeding Research

There are multiple studies investigating tritium breeding based on the reaction of lithium with neutrons. Some of the more prominent studies will be reviewed here.

Most of these studies are focused on breeding during fusion operation, thus it is important to produce more tritium than is burned, to account for issues of efficiency. Thus, the term *Tritium Breeding Ratio* (TBR) must be greater than one.

The TBR is defined as the number of tritium bred relative to the number of neutrons produced by the D-T fusion reaction.

2.5.1 The LIBRA Experiment

LIBRA stands for (*Liquid Immersion Blanket: Robust Accountancy*) It is an experiment by MIT Plasma Science and Fusion Center [18]. It was designed based on the ARC (Affordable, Robust, and Compact) tokamak design to simulate a very simple setting for a Liquid Immersion Blanket (LIB) while changing the required parameters to achieve $TBR > 1$.

2.5.1.1 Arc tokamak

The ARC tokamak is a conceptual compact high magnetic field tokamak for research purposes [19], to demonstrate a fusion power plant and study nuclear fusion science. A schematic of ARC tokamak reflects the possible final size shown in **Figure 2.3**.

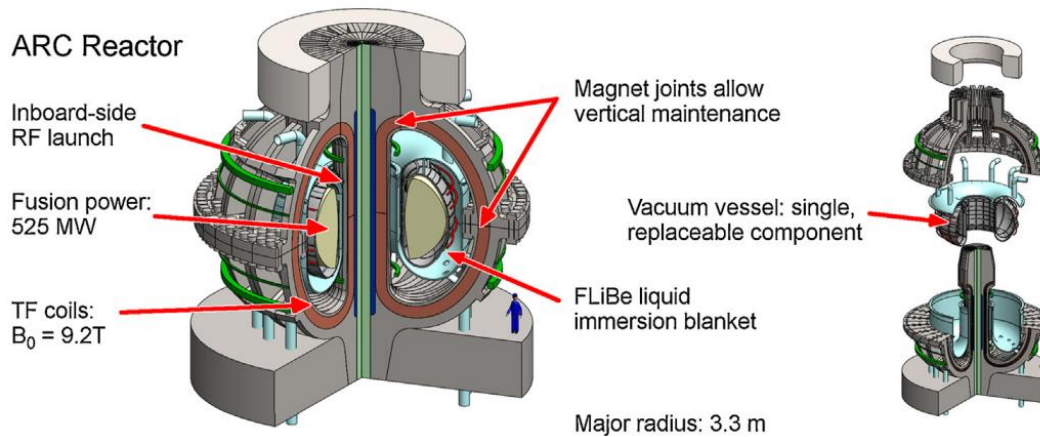


Figure 2.3. Arc schematic [19].

2.5.1.2 Liquid Immersion Blanket

This study relies on a simple molten-FLiBe-salt (Fluoride-Lithium-Beryllium) tritium breeding blanket. LIBRA simulates a blanket environment using open-MC and generates neutrons based on the energy spectrum of the neutrons released from D-T fusion.

According to reaction (1.37) the total output energy is 17.6 MeV; the neutron energy is expected to be about 14 MeV, and according to **Figure 2.2**, the LIBRA experiment relies on ${}^7\text{Li}$ interacting with neutrons [18].

The experiment also tested the thickness required to maintain the correct neutron energy spectrum. In addition, it made a comparison with FLiNaK LIB, where it concluded FLiNaK requires a much bigger thickness, consequently, affecting the neutron energy spectrum. This is due to the presence of beryllium in FLiBe, which acts as neutron multiplier and enhances tritium breeding.

A schematic of the LIBRA experiment shown in **Figure 2.4**.

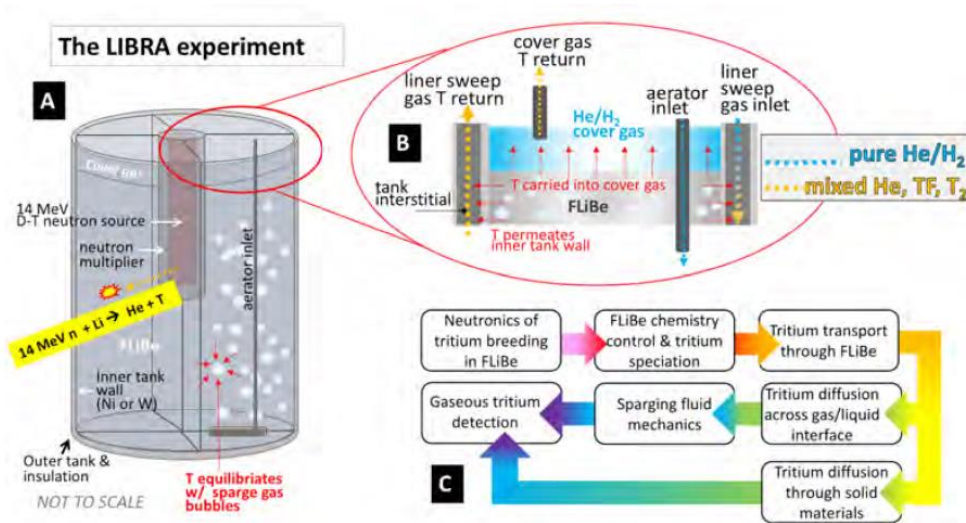


Figure 2.4. (A) A D-T neutron generator is surrounded by a cylindrical tank of FLiBe (~1m diameter). (B) Tritium is carried to the detection system via the cover gas or via liner sweep gas return. (C) LIBRA process [18].

The LIBRA experiment is still ongoing. So far, Phase I used Open-MC simulations to determine the minimum radial thickness of FLiBe LIB needed, the result is about 40 cm [18].

Figure 2.5 shows the output of an Open-MC simulation of the LIBRA system. It also shows that the TBR is above unity when the blanket thickness is above 50 cm. The 10^{10} n/s neutron source is located at the center of the cylindrical tank and surrounded by a 5 cm Pb layer for a neutron multiplication boost [18].

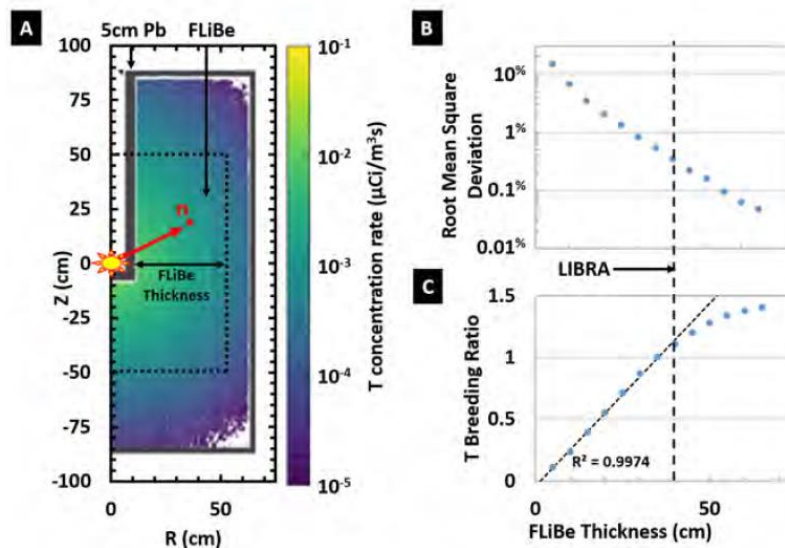


Figure 2.5. (A) Schematic of the cylindrical LIB cross-section. (B) RMS deviation in neutron energy spectra is plotted as a function of FLiBe thickness. (C) LIBRA TBR is plotted as a function of FLiBe thickness [18].

2.5.2 ITER Tritium Breeding Module

ITER is an international project located in southern France. There are numerous collaborative studies competing to be the applied solution for tritium breeding. This review will include one of the studies that achieved the preliminary design stage [2].

2.5.2.1 Chinese Helium Cooled Ceramic Breeder Test Blanket System (HCCH TBS)

The Chinese (HCCB-TBS) is the first Test Blanket System to enter its preliminary design phase for ITER [2].

This experiment uses lithium orthosilicate (Li_4SiO_4) pebbles as the tritium breeder, beryllium pebbles as neutron multiplier, and pressurised Helium (8 MPa)

to cool the pebbles (lithium orthosilicate and beryllium) [20]. The following

Figure 2.6 gives an illustration of all the components.

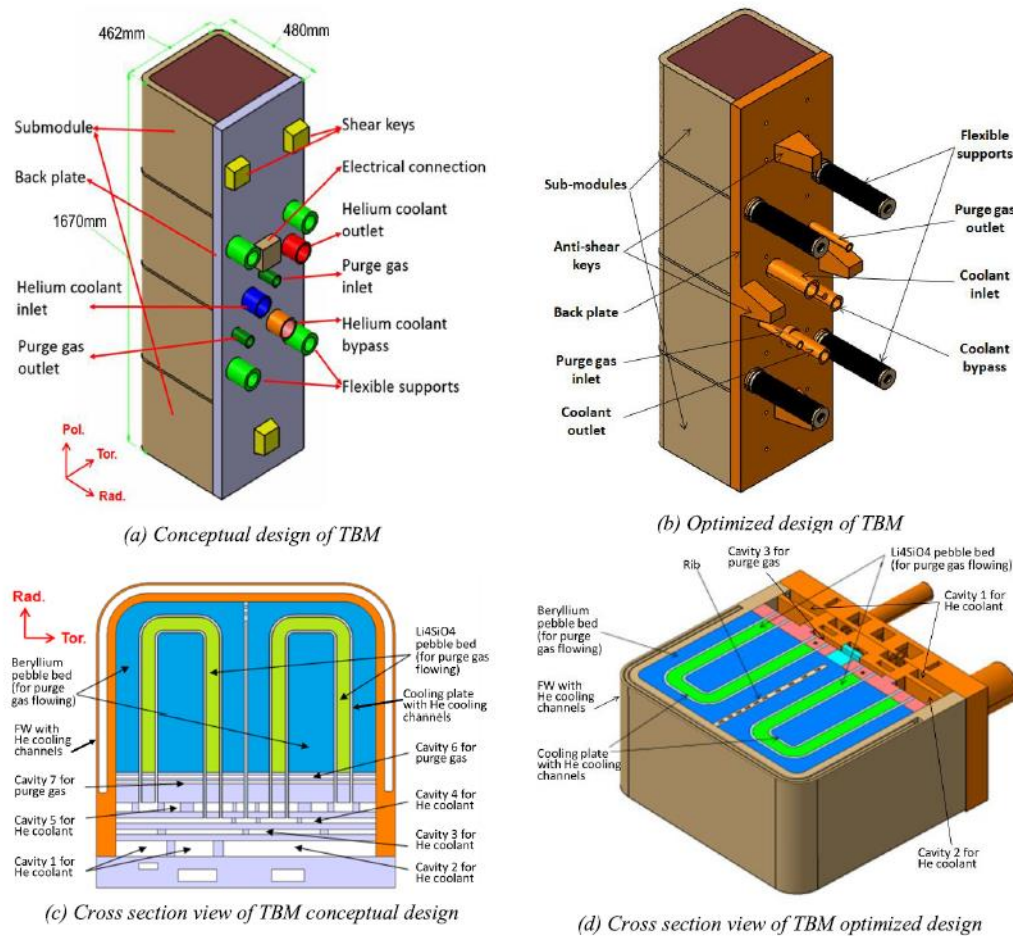


Figure 2.6. HCCB TBS design optimization of the TBM [20].

Although this study did not clearly indicate the anticipated TBR value, it uniquely incorporates the heat exchanging within the breeding system. The (HCCB TBS) relies on the same neutron energy spectrum as the LIBRA experiment.

2.6 Role of Molten Salt Reactor.

The concurrent studies into tritium breeding rely on a successful nuclear fusion ignition to breed the tritium and sustain the continuity of the reaction. The previously mentioned tritium breeding studies share the following aspects:

Neutron energy spectrum. Tritium breeding during fusion relies on the D-T neutron energy spectrum as shown in **Figure 2.7** [21], which is above 10 MeV.

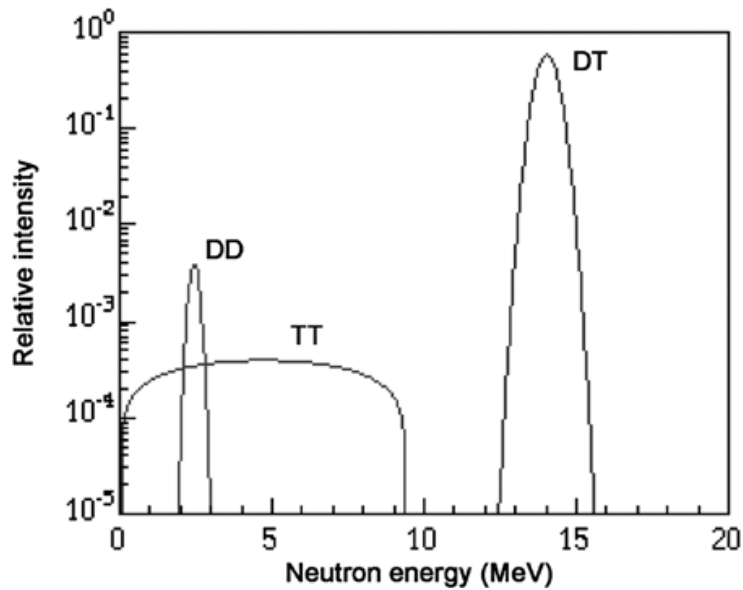


Figure 2.7. Normalized neutron energy spectra for DD, TT, and DT fusion [21].

Lithium in blanket. Lithium represents the main element for breeding tritium, either used within a liquid molten salt like the LIBRA experiment or within a ceramic like the (HCCB) project. However, according to **Figure 2.2**, it is ^7Li that will matter.

Neutron multiplier. During fusion energy tritium breeding benefits from the neutron energy spectrum and can use beryllium and lead as neutron multipliers.

However, before we ignite any fusion reaction, enough tritium is needed to satisfy Lawson's criterion, and until tritium breeding during fusion is improved enough to achieve $TBR > 1.2$ [18], tritium reserves are needed every time a nuclear fusion reaction is restarted. Thus, securing a tritium supply will speed up progress toward nuclear fusion.

The Molten Salt Reactor was chosen for this study because lithium is one of the elements in the molten salt fuel/coolant.

Chapter 3

Methodology

3.1 MSR, General introduction

All current research projects rely on the Molten Salt Reactor Experiment (MSRE) at ORNL which was operated between 1965 to 1969 and where the salt used was a specific combination of lithium fluoride and beryllium (FLiBe) [22].

3.1.1 MSRE's Fuel and Coolant Mixture

The fuel salt used in MSRE at ORNL is presented in **Table 3.1**. Where, ^{235}U enrichment is about 32% [23].

Table 3.1. MSRE Molten Salt Fuel Mixture [23].

Fuel Salt Component	Compositions	
	Mole %	Weight %
LiF	65	40.48
BeF ₂	29.1	32.76
ZrF ₄	5.0	20.02
$^{238}\text{UF}_4$	0.61	4.59
$^{235}\text{UF}_4$	0.29	2.16

The mixes were selected based on their nuclear, chemical, and physical properties to create an eutectic¹³ mixture based on the LiF-BeF diluent system. **Figure 3.1** below illustrates the phase diagram of this system.

¹³ A mixture is eutectic when it melts or solidifies at a temperature lower than any of its components.

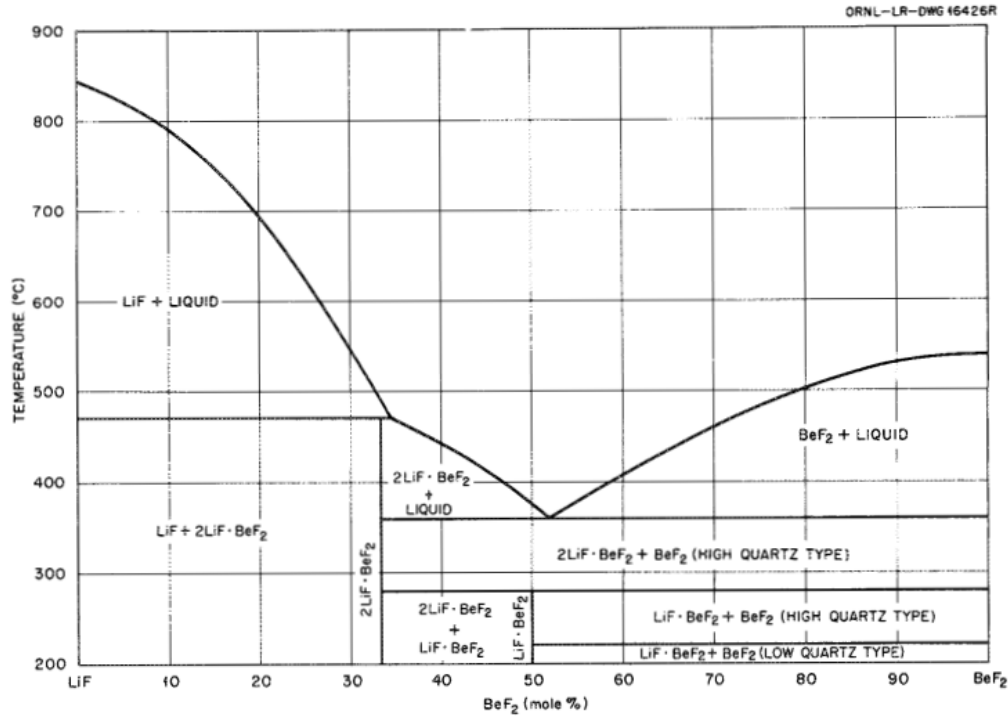


Figure 3.1. LiF-BeF₂ diluent system [23].

The secondary coolant was a simple mixture of LiF and BeF₂, as illustrated in

Table 3.2.

Table 3.2. ORNL Molten Salt Secondary Coolant Mixture [23].

Blanket Salt Component	Compositions	
	Mole %	Weight %
LiF	66	51.78
BeF ₂	34	48.22

3.1.2 Neutron Economy and the Choice of Salt

The nuclear property is one of the important considerations for selecting the appropriate salt. Lithium beryllium fluoride salt was chosen because of the small cross section for ⁷Li ($\sigma_{\text{thermal}}=0.045$ barn) and Be ($\sigma_{\text{thermal}}=0.0088$ barn) when interacting with thermal and epithermal neutrons [24]. Molten chloride salts have

been proposed for fast reactors because the neutron absorption cross-section of ^{35}Cl is small for fast neutrons ($\sigma_{\text{fast}} = 0.0011$ barn, $\sigma_{\text{thermal}} = 43.63$ barn) [24]. Thus, these choices were made according to the neutron energy spectrum to lower the effect on neutron population.

It is important to recognize that in MSRE, beryllium does not act as a neutron multiplier because the neutrons are moderated, and its energy is lower than the threshold for neutron interaction.

3.1.3 Lithium in MSRE

Although the melting point is the most significant physical property for a coolant in selecting an eutectic mix to fit the requirements [25], reducing corrosion is also an important consideration. Corrosion of metals in molten salt reactors is related to the electrochemical charge-transfer on the metal-electrolyte interface which is dependant on the mass-transfer of involved species across the boundary [25], and therefore related to the mass transfer rate of the chosen molten salt.

Usually, the best choice regarding corrosion is that with lowest “redox potential”, which is a measurement of the ability of a specific element to lose or gain an electron [26]. **Figure 3.2** below shows the redox potential as a function of temperature for multiple fluoride salts. The salt with highest lithium percentage has the lowest redox potential, and so will have the lowest electrochemical charge and mass transfer choice. Thus, FLiBe is considered the best choice to lower the effect of corrosion.

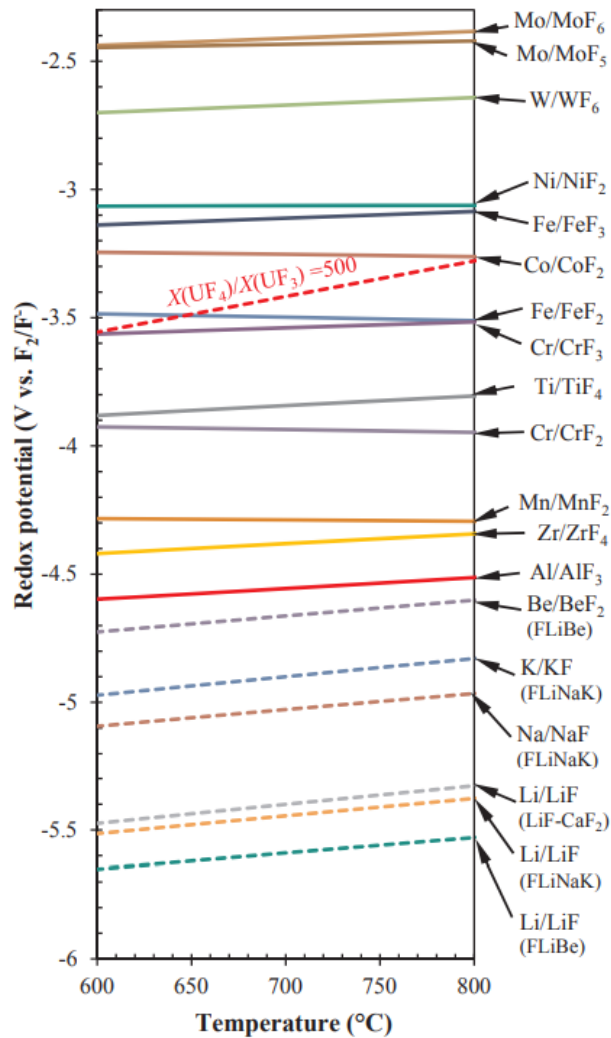


Figure 3.2. Redox potentials of various redox couples as a function of temperature in fluoride salts. Solid line: metal dissolution. Dotted line: reduction of oxidants [24].

Thus, lithium in the molten salt, has an important role in preventing corrosion. However, as mentioned in “Sec 2.2”, lithium has two stable isotopes (${}^6\text{Li}$ 7.5%, and ${}^7\text{Li}$ 92.5 %), with ${}^6\text{Li}$ having a very high cross section for thermal neutrons, which would consequently affect neutron population. Therefore, MSRE used lithium 99.99 % ${}^7\text{Li}$ enriched [23].

3.2 MCNP4C

Since it is not possible to create the experiment physically within a short time frame, it was emulated using MCNP4C code.

MCNP is a Monte Carlo N-Particle code that can be used for neutron, photon, electron, or coupled neutron/photon/electron transport, including the capability to calculate eigenvalues for critical systems.

MCNP4C was chosen because it has features that make it very versatile and easy to use. It has an extensive collection of cross-section data. It can generate detailed geometry and output tally plotters; a flexible tally structure; also, a variety of output tables to analyse the data [27].

3.3 Method

3.3.1 Experiment Setting and Design

A simple arrangement of a molten salt reactor was created after multiple trial arrangements were tested until criticality was achieved ($k_{eff} = 1$). A set of 61 fuel channels was arranged hexagonally in a graphite moderator within a cylinder, and a molten salt blanket with variable thickness as shown in **Figure 3.3**.

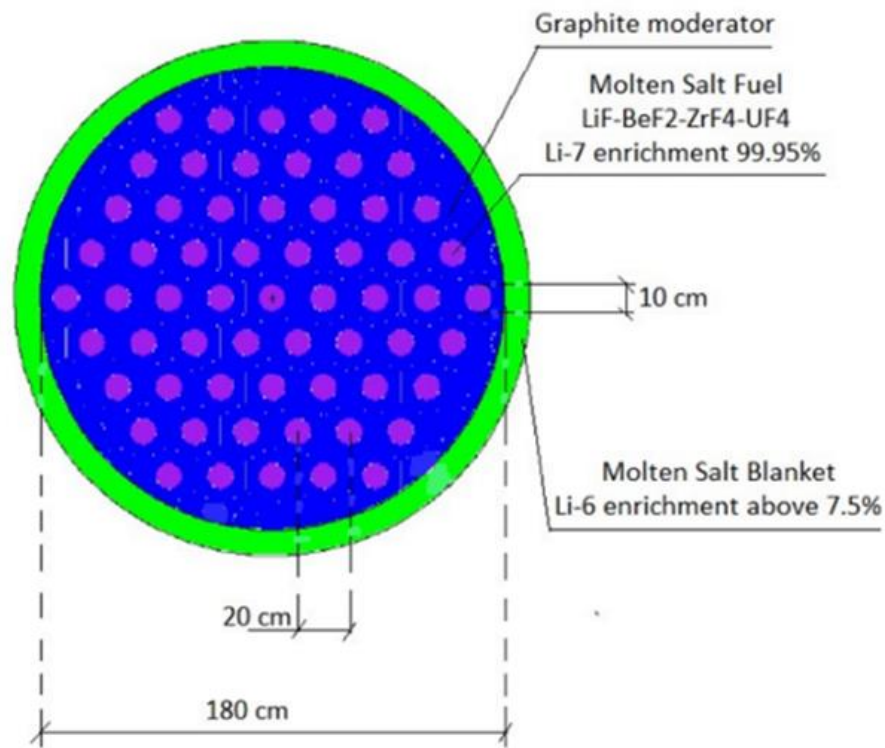


Figure 3.3. Cross section of Simple Molten Salt Reactor arrangement. Figure created using MCNP4C.

3.3.1.1 Fuel selection

The eutectic mixture is chosen to be the same as the fuel mixture for MSRE [23], except a) To make this study a reference for future civil purpose research, ^{235}U enrichment should not exceed 20%. b) ^7Li enrichment is 99.95%. **Table 3.3** lists the molar distribution. The density was taken to be 3.06 g/cm^3 .

Table 3.3. Experiment Molten Salt Fuel Mixture.

Fuel Salt Component	Compositions	
	Mole %	Weight %
LiF	65	40.48
BeF ₂	29.1	32.76
ZrF ₄	5.0	20.00
²³⁸ UF ₄	0.72	5.42
²³⁵ UF ₄	0.18	1.34

3.3.1.2 Blanket Molten Salt

Like the fuel, the molten salt in the blanket is based on the eutectic mixture for the MSRE secondary coolant, however the ⁶Li removed from the fuel mixture is added to the blanket. Thus, the blanket will use enriched ⁶Li above the natural 7.5%. This enrichment will depend on the thickness of the blanket and be called the optimal level. The density of the salt chosen is 1.94 g/cm³ according to the density at 700 °C [25].

Optimal level: it is a term used in this document referring to the enrichment of ⁶Li in the blanket above 7.5%, after removing ⁶Li from the fuel salt.

3.3.2 The Process

3.3.2.1 Calculation of Elements Weight Distribution

To use MCNP4C, it is important to insert the correct weight distribution to comply with the eutectic mix for each fuel molten salt mix, and the blanket molten salt mix.

Assuming an element X makes $r\%$ mole of a total mix with density ρ , then the weight distribution of element X can be calculated according to the following equation:

$$X_{weight} = \frac{X_{molar\ weight} \times r}{total\ mix\ molar\ weight} \quad 3.1)$$

All the compounds listed contain fluoride which means the fluoride entry in **Table 3.4** is the sum of the fluoride in all of the compounds. It is also important to remember that ${}^6\text{Li}$ and ${}^7\text{Li}$ enrichment will reflect on the weight distribution.

Thus, for the fuel mixture¹⁴ the elements weight distribution is listed in **Table 3.4**.

Table 3.4. Experiment fuel mix – Elements weight distribution per 1 gram.

Element	${}^{235}\text{U}$	${}^{238}\text{U}$	${}^6\text{Li}$	${}^7\text{Li}$	Be	Zr	F
Weight	0.01013	0.04105	0.00005	0.10893	0.06273	0.10899	0.66812

For the blanket, the distribution of ${}^6\text{Li}$, and ${}^7\text{Li}$ changes according to the thickness and the optimal level of ${}^6\text{Li}$ enrichment, which we will see in the next chapter.

3.3.2.2 Assumptions.

MCNP4C has restrictions which forced the following assumptions to be made:

- The temperature and temperature distribution are ignored,
- Refuelling is not considered, (as is the case for most molten-salt reactors).

These assumptions will have a consequence on fuel design issues like density, fuel burnup, and neutron population, which are not discussed in detail in this document.

¹⁴ See input file (input A) example, fuel salt is (m1). Appendix B

The purpose of these assumptions was to simplify the study, while focusing on analysing the effect of the blanket, and the enrichment of ${}^6\text{Li}$ on tritium production.

Chapter 4

Results and Verification

4.1 Introduction – MCNP4C Data Collection Tools

MCNP4C provides multiple tools for analysis. It is important to select a tool that allows data collection to follow the same patterns and allow data comparison.

This document relies on output (table 140), which will contain information like total collisions, collisions*weight, weight lost to capture etc. from which we can extract the reaction rate and energy.

4.2 Data Collection and Observation

Since applying the blanket is essential to tritium production in this study because of the increased ${}^6\text{Li}$ enrichment (optimal level), the optimal blanket thickness must first be found. Then the effect of changing ${}^6\text{Li}$ enrichment in the blanket away from the proportional value can be investigated. Thus, the data was collected in two stages.

4.2.1 Stage 1 – Finding the optimal thickness.

For the same number of fuel channels, (in this case 61), four blankets were applied in turn, thickness 20 cm, 15 cm, 10 cm, and 5 cm. The MCNP4C files are

named A, B, C, and D accordingly. **Table 4.1** summarises the MCNP4C files, thickness and the proportional ${}^6\text{Li}$ enrichment¹⁵.

Table 4.1. MCNP4C files with blanket thickness, and ${}^6\text{Li}$ optimal level enrichment.

MCNP4C file	61 fuel Channels	
	Thickness cm	${}^6\text{Li}$ %
A	20	10.55
B	15	11.79
C	10	14.29
D	5	21.91

Thus, for blanket thickness 20 cm, the weight distribution in the blanket molten salt mix¹⁶ is listed in **Table 4.2**.

Table 4.2. Blanket 20 cm thickness - elements weight distribution per 1 gram.

Element	${}^6\text{Li}$	${}^7\text{Li}$	Be	F
Weight	0.014730	0.124850	0.091103	0.769317

As explained earlier, (table140)¹⁷ is used, to calculate the reaction rate in ${}^6\text{Li}$ and ${}^{235}\text{U}$. Also, to check the criticality. The process is repeated for file B, C and D.

The output is summarized in **Figure 4.1**. Although, the output data shows that tritium produced increases in proportion to the thickness, this is related to the number of ${}^6\text{Li}$ interactions with the neutrons, however this increase is practically negligible. Meanwhile, an optimal range of blanket thickness in relation to criticality ($k_{\text{eff}} = 1$) can be observed.

¹⁵ The proportional enrichment for each case was calculated using (excel) taking into consideration the geometry, and the design setting.

¹⁶ See input file (input A) example, fuel salt is (m3). Appendix B

¹⁷ See output file (output A) example. Appendix B

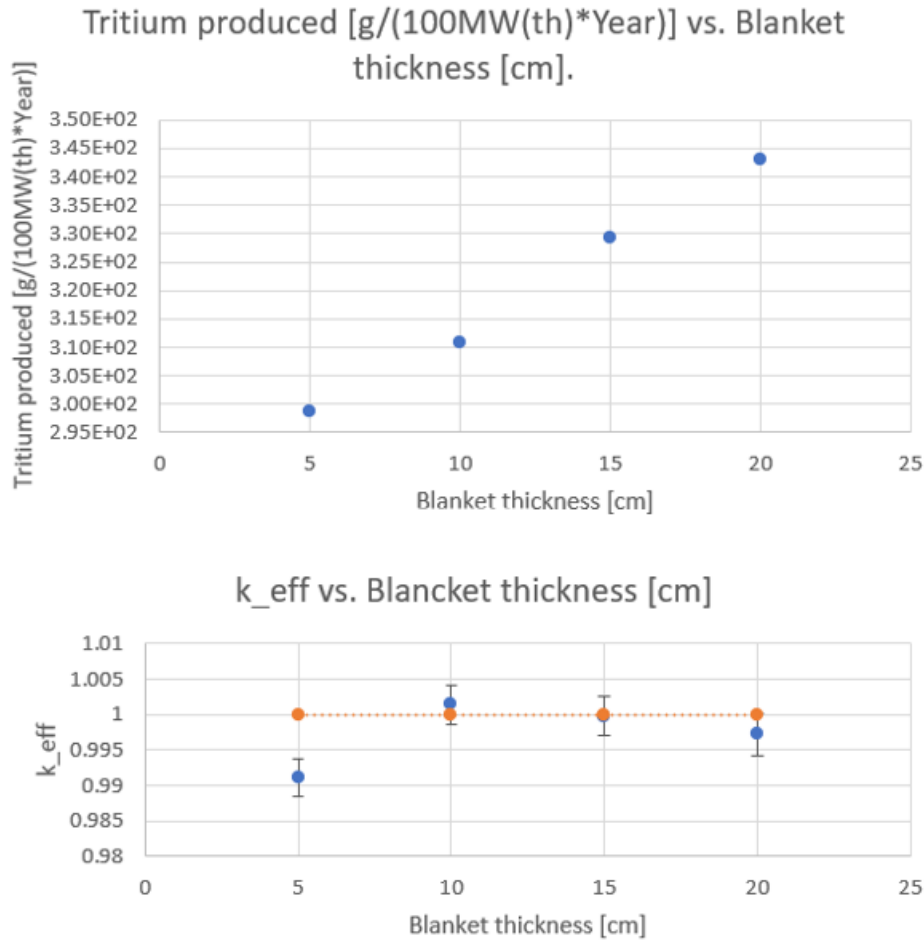


Figure 4.1. Data based on MCNP4C output for four blanket thickness/proportional ⁶Li enrichment.

The optimal thickness ranges between 10 cm to 15 cm (File B & C), where the reactor is considered critical.

4.2.2 Stage 2 – Effect of ⁶Li enrichment in a fixed thickness in the blanket

To investigate the effect of ⁶Li enrichment, the thickness of the blanket is fixed, and the enrichment is either increased or reduced from the optimal level. Thus, case B was chosen because it is one of the two cases within the optimal thickness range. ⁶Li enrichment is changed according to **Table 4.3**.

Table 4.3. MCNP4C file with variable ⁶Li enrichment.

61 fuel channels – 15 cm thick blanket									
MCNP file	BA	BB	BC	BD	BE	BF	BG	BH	BI
⁶ Li Enrichment [%]	8	9	10	11	11.79	13	14	15	16

The results are summarized in **Figure 4.2**, showing that the criticality of the reactor is affected, and the best output is at the original enrichment level of 11.79%.

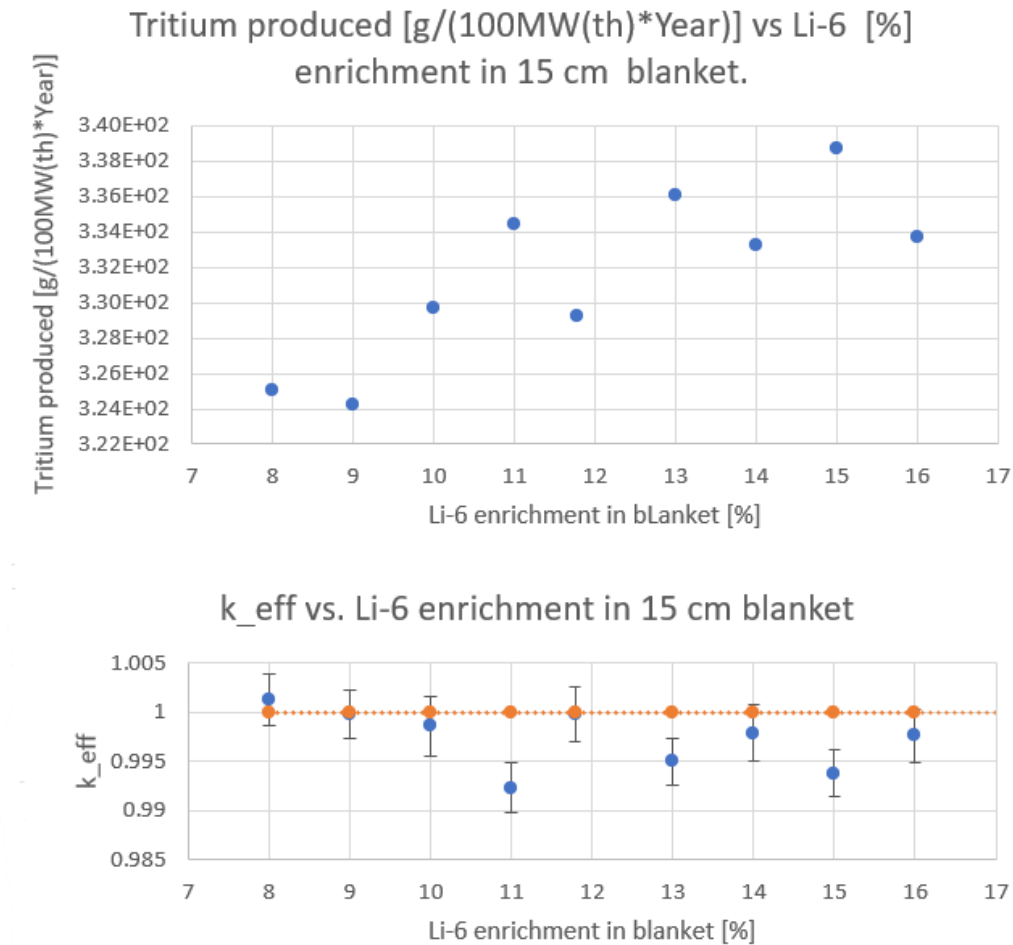


Figure 4.2. Data based on MCNP4C output for different ⁶Li enrichment level in the blanket.

4.2.3 Data summary and observations

Based on Stage -1 observations, the expected average value of tritium produced is $325 \text{ g year}^{-1}/(100 \text{ MW (th)})$, which is more than double the tritium produced annually by a CANDU reactor.

Also, based on Stage -2, it appears most efficient to start by finding the optimal blanket thickness, then use the corresponding proportional enrichment level for ${}^6\text{Li}$. This simplifies the design process.

4.3 Verification and benchmarking

To verify the accuracy of the results, two methods of benchmarking were followed, a) Identifying ${}^6\text{Li}$ cross section using MCNP4C and comparing the results with National Nuclear Data from the Brookhaven database. b) Comparing tritium produced with ORNL results.

4.3.1 Identifying ${}^6\text{Li}$ cross section using MCNP4C

As illustrated in (Chapter 2. Sec 2.2), ${}^6\text{Li}$ is the isotope of interest. Thus, the verification process relied on verifying the ${}^6\text{Li}$ cross section.

To accomplish this, a testing cell composed of a 0.3 cm high cylinder with 4 cm radius was arranged, the cylinder was filled with ${}^6\text{Li}$ with density of 0.0167 [atoms/barns.cm]. The sample was then bombarded with 1 million evenly distributed neutrons in a beam (Monodirectional disk source). The MCNP4C test

was run multiple times with each run choosing a different neutron energy level¹⁸ starting from 15 keV to 2.6 MeV. This arrangement is represented in **Figure 4.3** below.

Then, the reaction rate was calculated, and the process applied according to the methods shown in (Sec 1.3.1.2) using equation (1.25) to calculate the cross section. The output was compared with the data of National Nuclear Data Center (NNDC) from the Brookhaven database [7].

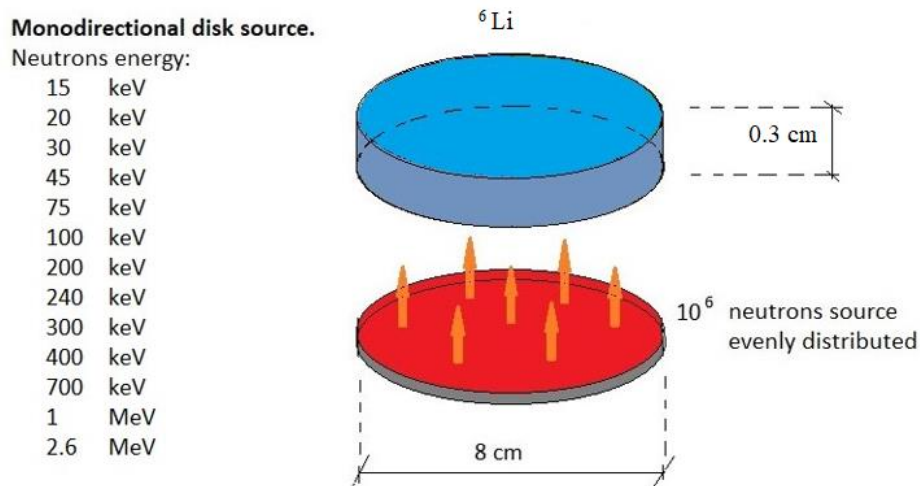


Figure 4.3. Test cell. A test was run for each listed energy level.

Table 4.4 lists the values of ⁶Li cross section in [barn] verses the energy in [MeV] as taken from NNDC.

Table 4.4. ⁶Li cross section at specific neutron energy from NNDC.

E [MeV]	0.015	0.020	0.030	0.045	0.075	0.100	0.200
σ [barn]	1.2301	1.0737	0.893	0.7562	0.6532	0.6515	1.9653
E [MeV]	0.240	0.300	0.400	0.700	1.000	2.600	
σ [barn]	3.2568	1.4743	0.5591	0.2740	0.2297	0.1879	

¹⁸ See output file for the case of E=0.3 MeV. See Appendix B.

Figure 4.4 shows the calculated cross section for ${}^6\text{Li}$ using MCNP4C. When this is compared with the values from **Table 4.4**, the error was presented showing a maximum relative error of 5%.

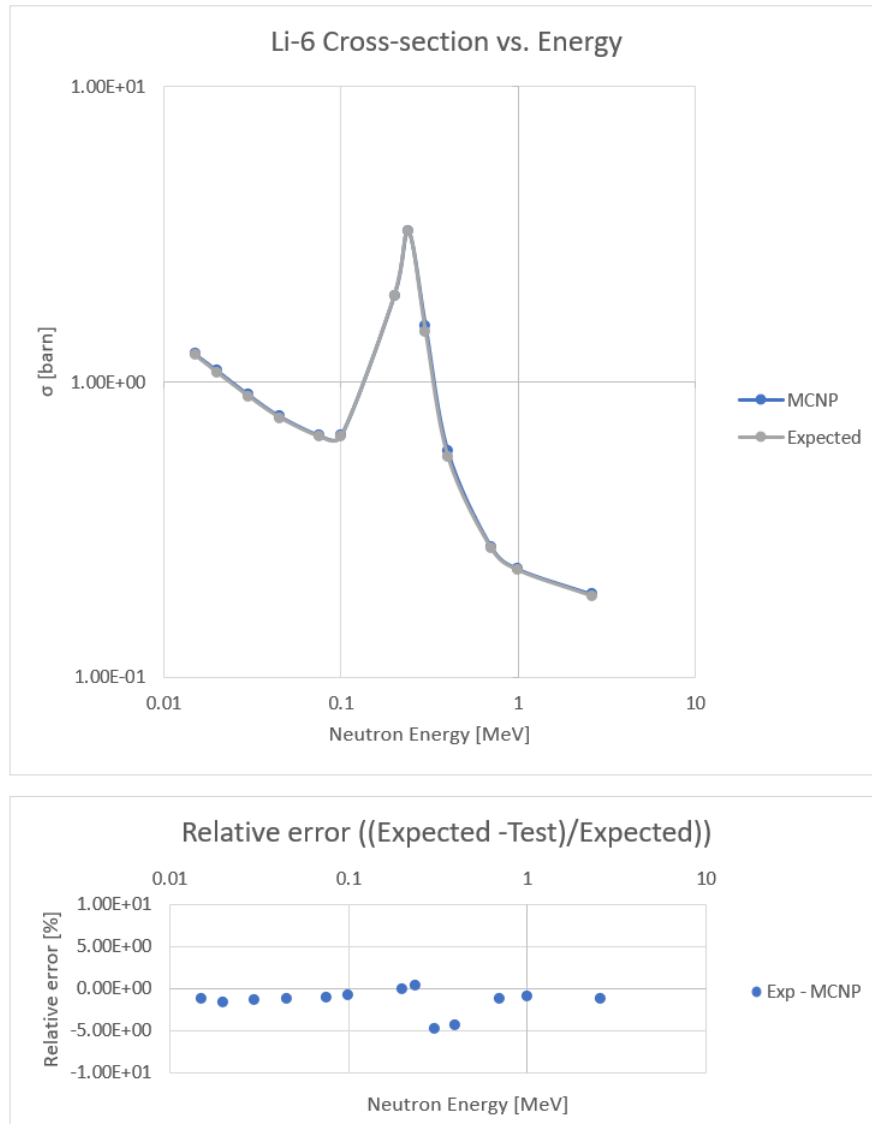


Figure 4.4. ${}^6\text{Li}$ cross section as calculated using MCNP4C, and relative error.

4.3.2 Benchmarking – Comparison with ORNL results.

A simplified critical MSR with 19 fuel channels was created. The fuel salt for this case was 32% ^{235}U enriched, and 99.99% ^7Li enriched. This setting was based on the original MSRE values (Sec 3.1.1) and (Sec 3.1.3). with no molten salt blanket

Figure 4.5 below shows a top view cross section of the setting.

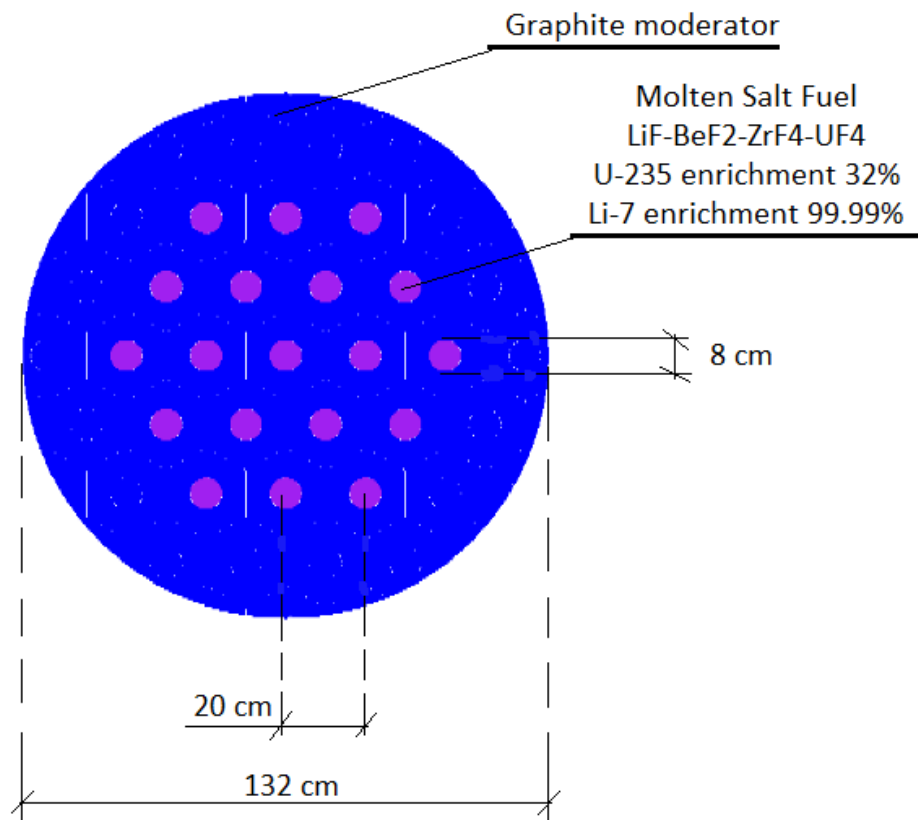


Figure 4.5. Top view cross section of simple molten salt reactor arrangement for ORNL Benchmarking. Figure created using MCNP4C.

The tritium produced in [Ci/(day.MW(th))] was calculated for the purpose of comparison with ORNL data [28]. MCNP4C was used to calculate the tritium produced based on the reaction rate process¹⁹.

Using the half life of tritium (12.33 years) with equation (A. 4)²⁰ gives tritium production of 7.3 Ci/(day.MW(th)) or 27.8 g/(year.100 MW (th)). This closely approximates the ORNL results of 7.4 Ci/(day.MW(th)) [28], within 1%.

4.3.3 Verification Summary

Since the same assumptions and considerations were applied to the verification, the results from the two steps of verification, show that despite the assumption and simplification used, the output data hold a good level of accuracy.

¹⁹ See output file for ORNL Benchmarking. Appendix B

²⁰ See sec A-2 (Radioactivity Measurement). Appendix A

Chapter 5

Conclusion and Recommendation.

5.1 Conclusion

Although the results contained in this study are based on simulations with limitations imposed by the required assumptions, they indicate that it would be possible to use current technology in nuclear fission reactions to increase tritium production, (in this instance from molten salt reactors).

The amount of tritium produced annually from the sample reactor falls short of fully fuelling a fusion reactor. However, it can provide the tritium required to ignite a fusion reactor. This potentially enables successful breeding during the fusion reaction and opens the door to the possibility of a hybrid of fission-fusion technology. The tritium produced is also more than double the amount produced by the current primary tritium producing reactor – the CANDU – and for a smaller reactor.

A possible integration of fission-fusion as a source of energy, will not only make achieving fusion sooner a possibility, but it will also move us closer toward a future without the need for carbon fuels while using less fission fuel.

5.2 Recommendation

This study relied on ORNL document for MSRE, which is considered a thermal reactor, so ${}^6\text{Li}$ was the element of interest, and this reduced the possibility of using Be as a neutron multiplier.

However, this outcome shows that it is possible to breed tritium from different fission technology. In a fast reactor as an example, it would be possible to use Be as a neutron multiplier, in the meantime there is no need for lithium enrichment, since in high energy spectrum, ${}^7\text{Li}$ cross section for tritium production starts to increase.

It also bears mentioning that further study is needed for scenarios with higher burnups and different temperatures.

Appendix A Elements Classification and Radioactivity

A.1 Periodic Table.

The Periodic table in **Figure A. 1** below, classifies elements into groups based on Z (the number of protons within the nucleus).

Periodic table of the elements

Legend:

- Alkali metals
- Alkaline-earth metals
- Transition metals
- Other metals
- Other nonmetals
- Halogens
- Noble gases
- Rare-earth elements (21, 39, 57-71) and lanthanoid elements (57-71 only)
- Actinoid elements

group 1*	2	3	4	5	6	7	8	9	10	11	12	13	14	15	16	17	18
1	2	3	4	5	6	7	8	9	10	11	12	13	14	15	16	17	18
1	2	3	4	5	6	7	8	9	10	11	12	13	14	15	16	17	18
1	2	3	4	5	6	7	8	9	10	11	12	13	14	15	16	17	18
2	3	4	5	6	7	8	9	10	11	12	13	14	15	16	17	18	19
2	3	4	5	6	7	8	9	10	11	12	13	14	15	16	17	18	19
3	4	5	6	7	8	9	10	11	12	13	14	15	16	17	18	19	20
3	4	5	6	7	8	9	10	11	12	13	14	15	16	17	18	19	20
4	5	6	7	8	9	10	11	12	13	14	15	16	17	18	19	20	21
4	5	6	7	8	9	10	11	12	13	14	15	16	17	18	19	20	21
5	6	7	8	9	10	11	12	13	14	15	16	17	18	19	20	21	22
5	6	7	8	9	10	11	12	13	14	15	16	17	18	19	20	21	22
6	7	8	9	10	11	12	13	14	15	16	17	18	19	20	21	22	23
6	7	8	9	10	11	12	13	14	15	16	17	18	19	20	21	22	23
7	8	9	10	11	12	13	14	15	16	17	18	19	20	21	22	23	24
7	8	9	10	11	12	13	14	15	16	17	18	19	20	21	22	23	24
lanthanoid series 6	58	59	60	61	62	63	64	65	66	67	68	69	70	71			
lanthanoid series 6	58	59	60	61	62	63	64	65	66	67	68	69	70	71			
actinoid series 7	90	91	92	93	94	95	96	97	98	99	100	101	102	103			
actinoid series 7	90	91	92	93	94	95	96	97	98	99	100	101	102	103			

*Numbering system adopted by the International Union of Pure and Applied Chemistry (IUPAC). © Encyclopædia Britannica, Inc.

Figure A. 1. Periodic table [29].

Actinoid elements. These are elements comprised of 15 consecutive elements starting with actinium ($Z=89$) and ending with lawrencium ($Z=103$). Most of these elements are man made as they contain 11 of the transuranium elements [29].

Transuranium elements: these are elements that have an atomic number Z bigger than that of uranium ($Z=92$). All transuranium elements are artificially produced except for some trace of plutonium found in naturally occurring uranium. Some of these elements have a very long life like the neptunium isotope ^{237}Np which releases 5 MeV alpha particles [29].

Lanthanide element. These elements are named after lanthanum because chemically they behave similarly [29].

A. 2 Radioactivity measurement

Unstable elements decay emitting gamma, beta, and alpha radiation. The energy carried with these radiations can cause harm to humans and animals. However, in nature there are multiple sources of radiation that humans and animals have been living with since the beginning of life on earth. Therefore, it is important to create a unit for measuring the amount of radioactivity to assign regulations and protection.

Curie: Is the original unit of measuring radioactivity (Ci), having an exact value of $1 \text{ Ci} = 3.7 \times 10^{10}$ decay per second [5]-(Sec 6.1).

Becquerel: The International System of Units (SI) [5]-(Sec 6.1), replaced the curie with the becquerel (Bq), $1 \text{ Bq} = 1$ decay per second, thus, $1 \text{ Bq} = 2.703 \times 10^{-11} \text{ Ci}$.

However, it is important to recognize that both curie and becquerel measure only the number of disintegrations occurring per unit of time, and do not measure the amount of energy released per disintegration. The energy release measurement follows another related unit which is beyond the scope of this document.

Decay rate calculation:

It is known that any radioactive substance decays exponentially. So, if we have N radioactive nuclei at a time t , then the number of disintegrating nuclei in a time dt is proportional to N , as expressed in “equation(A. 1)”.

$$\left(\frac{dN}{dt}\right)_{decay} = -\lambda N \quad (\text{A. 1})$$

Where λ is the decay constant, which is directly related to the half-life $t_{1/2}$. The half-life is the time required for the decay of half of the initial mass N_0 , then by integrating dN/dt we get the exponential law of radioactive decay according to “equation **Error! Reference source not found.**” [5] (Sec 6-1).

$$N(t) = N_0 e^{-\lambda t} \quad (\text{A. 2})$$

Therefore, for $N(t) = 0.5 N_0$,

$$t_{1/2} = \frac{0.693}{\lambda} \rightarrow \lambda = \frac{0.693}{t_{1/2}} \quad (\text{A. 3})$$

Thus, the reactivity rate can be calculated using “equation **Error! Reference source not found.**” with [seconds] as the unit for the half-life. Thus, for one gram of a radioactive element, the calculated rate in [becquerel] is:

Reactivity per 1 gram of matter

$$= \frac{0.693}{t_{1/2} [\text{second}]} \frac{6.02 \times 10^{23} \left[\frac{\text{atoms}}{\text{mole}} \right]}{A \left[\frac{\text{grams}}{\text{mole}} \right]} \quad (\text{A. 4})$$

Appendix B Data and MCNP4C Code samples

B.1 Input File example

File input A: 20 cm thickness blanket

```

MSR with 20cm thk Blanket 61 fuel road h=200cm 10.55 % Li-6 in Blanket
c -----
c < Cell Section >
c Fuel
111 1 -3.05605 -10 u=1 imp:n=1 $ Fuel
112 2 -1.75000 10 u=1 imp:n=1 $ Moderator (graphite)
c 113 2 -1.75000 11 u=1 imp:n=1 $ Moderator (graphite)
c Non-fuel element, ie moderator
121 2 -1.75000 -10 u=2 imp:n=1 $ Empty cell, graphite
122 2 -1.75000 10 u=2 imp:n=1 $ Empty cell, graphite
c 123 2 -1.75000 11 u=2 imp:n=1 $ Empty cell, graphite
c Lattice of universes 1 and 2
500 0 -100 u=3 imp:n=1 lat=2
fill= -9:9 -9:9 0:0 $ Lattice
2 2 2 2 2 2 2 2 2 2 2 2 2 2 2 2 2 2 2 2 2 2
2 2 2 2 2 2 2 2 2 2 2 2 2 2 2 2 2 2 2 2 2 2
2 2 2 2 2 2 2 2 2 2 2 2 2 2 2 2 2 2 2 2 2 2
2 2 2 2 2 2 2 2 2 2 2 2 2 2 2 2 2 2 2 2 2 2
2 2 2 2 2 2 2 2 2 2 2 2 2 2 2 2 2 2 2 2 2 2
2 2 2 2 2 2 2 2 2 2 1 1 1 1 1 1 2 2 2 2 2 2
2 2 2 2 2 2 2 2 2 1 1 1 1 1 1 1 2 2 2 2 2 2
2 2 2 2 2 2 2 2 1 1 1 1 1 1 1 1 2 2 2 2 2 2
2 2 2 2 2 2 1 1 1 1 1 1 1 1 1 1 2 2 2 2 2 2
2 2 2 2 2 1 1 1 1 1 1 1 1 1 1 1 2 2 2 2 2 2
2 2 2 2 2 1 1 1 1 1 1 1 1 1 1 1 2 2 2 2 2 2
2 2 2 2 2 1 1 1 1 1 1 1 1 1 1 1 2 2 2 2 2 2
2 2 2 2 2 1 1 1 1 1 1 1 1 1 1 1 2 2 2 2 2 2
2 2 2 2 2 1 1 1 1 1 1 1 1 1 1 1 2 2 2 2 2 2
2 2 2 2 2 1 1 1 1 1 1 1 1 1 1 1 2 2 2 2 2 2
2 2 2 2 2 1 1 1 1 1 1 1 1 1 1 1 2 2 2 2 2 2
2 2 2 2 2 2 2 2 2 2 2 2 2 2 2 2 2 2 2 2 2 2
2 2 2 2 2 2 2 2 2 2 2 2 2 2 2 2 2 2 2 2 2 2
2 2 2 2 2 2 2 2 2 2 2 2 2 2 2 2 2 2 2 2 2 2
2 2 2 2 2 2 2 2 2 2 2 2 2 2 2 2 2 2 2 2 2 2
2 2 2 2 2 2 2 2 2 2 2 2 2 2 2 2 2 2 2 2 2 2
600 0 -300 -130 120 imp:n=1 fill=3 $ Core region with fuel
700 3 -1.94 -400 -130 120 #600 imp:n=1 $ Blanket, 2LiF-BeF2
1000 0 (400:130:-120) imp:n=0 $ Outside World
c -----
c Hex cell
100 rhp 0 0 -2 0 0 202 10.0 0 0
c 101 px 4.5 $ 1st side of the hexagonal lattice pin
c 102 2 px 4.5 $ 2nd side of the hexagonal lattice pin
c 103 3 px 4.5 $ 3rd side of the hexagonal lattice pin
c 104 4 px 4.5 $ 4th side of the hexagonal lattice pin
c 105 5 px 4.5 $ 5th side of the hexagonal lattice pin
    
```

```

c 106 6    px    4.5    $ 6th side of the hexagonal lattice pin
c -----
c The core
120      pz    0.0    $ Bottom of core
130      pz   200    $ Top of core
300      cz    90     $ Core radius
c -----
c The blanket
c 140     pz   -0.3    $ Bottom of blanket same as core
c 150     pz  150.3    $ Top of blanket same as core
400      cz   110     $ Radius, (outer radius)

c -----
c < Data Section >
c Coordinate Transformation for lattice cell edges
c *TR2  0 0 0      60 30 90      150 60 90      90 90 0 1
c *TR3  0 0 0      120 30 90     150 120 90     90 90 0 1
c *TR4  0 0 0      180 90 90     90 180 90     90 90 0 1
c *TR5  0 0 0      120 150 90    30 120 90     90 90 0 1
c *TR6  0 0 0      60 150 90    30 60 90      90 90 0 1
c -----
c Source Definition
kcode 1000 1.0 30 150
sdef pos=0 0 75 $ Release 14 MeV neutrons somewhere in the middle.
mode n
totnu
c -----
c m1 Molten Salt fuel
m1      92235.60c   -0.01013  $ U235, 20% enrichment
        92238.60c   -0.04105  $ U238
        3006.60c    -0.00005  $ Li-6
        3007.60c    -0.10893  $ Li-7, 99.95% enrichment
        4009.60c    -0.06273  $ Beryllium
        40000.60c   -0.10899  $ Zirconium
        9019.60c    -0.66812  $ Fluoride
c -----
c m2 is graphite moderator @ 300K *endf602*
m2      6000.60c   -1.0      $ C
mt2     grph.01t          $ Thermal Scattering
c -----
c m3 2LiF-BeF2 Blanket
m3      3006.60c   -0.014730  $ Li-6, 10.55 % enrichment
        3007.60c   -0.124850  $ Li-7,
        4009.60c   -0.091103  $ Beryllium
        9019.60c   -0.769317  $ Fluoride
c -----
c <Tallies>
FC4     Two Group Neutron Flux Tally in blanket
f4:n    700
E4      0.625e-6 1e-6 1e-5 1e-4 1e-3 1 2.5 100 $ Split flux 8 groups
SD4     1
FC14    Three Bins Neutron Flux Tally in Blanket
f14:n   700
fm14    (-1 3 -2) (-1 3 16) (-1 3 105) (-1 3 91)
SD14    1
print   140

c -----
print

```

B. 2 Output File Example

The output file for the MCNP4C is very long, thus the output example will include only (table 140) and (criticality summary box).

File output A: 20 cm thickness blanket – table 140

neutron activity of each nuclide in each cell, per source particle							print table 140
cell	nuclides	atom fraction	total collisions	collisions * weight	weight lost to capture	weight loss to fission	weight gain by (n,xn)
1	111	92235.60c	7.2959E-04	78774	5.5497E-01	8.6544E-02	5.7965E-06
		92238.60c	2.9192E-03	48898	3.6533E-01	8.6368E-02	1.9988E-05
		3006.60c	1.4072E-04	19383	1.3484E-01	1.3392E-01	0.0000E+00
		3007.60c	2.6283E-01	278362	2.1572E+00	1.1896E-02	0.0000E+00
		4009.60c	1.1783E-01	594873	4.5386E+00	4.2504E-03	0.0000E+00
		40000.60c	2.0225E-02	135711	1.0507E+00	8.9636E-03	7.8757E-06
		9019.60c	5.9532E-01	2153020	1.6647E+01	1.2657E-02	0.0000E+00
2	112	6000.60c	1.0000E+00	11101929	8.4962E+01	1.3622E-02	0.0000E+00
3	121	6000.60c	1.0000E+00	128634	9.8441E-01	1.7186E-04	0.0000E+00
4	122	6000.60c	1.0000E+00	562271	4.3087E+00	7.5957E-04	0.0000E+00
7	700	3006.60c	3.4565E-02	22675	1.6671E-01	1.5589E-01	0.0000E+00
		3007.60c	2.5118E-01	13947	1.0514E-01	4.9796E-05	0.0000E+00
		4009.60c	1.4269E-01	40110	3.0027E-01	1.1983E-04	3.0322E-04
		9019.60c	5.7157E-01	113916	8.5925E-01	3.2036E-04	0.0000E+00
total				15292503	1.1714E+02	5.1553E-01	8.5978E-03
total over all cells for each nuclide			total collisions	collisions * weight	weight lost to capture	weight loss to fission	weight gain by (n,xn)
		3006.60c	42058	3.0155E-01	2.8981E-01	0.0000E+00	0.0000E+00
		3007.60c	292309	2.2624E+00	1.1946E-02	0.0000E+00	0.0000E+00
		4009.60c	634983	4.8389E+00	4.3702E-03	0.0000E+00	8.5573E-03
		6000.60c	11792834	9.0255E+01	1.4553E-02	0.0000E+00	0.0000E+00
		9019.60c	2266936	1.7507E+01	1.2977E-02	0.0000E+00	6.7786E-06
		40000.60c	135711	1.0507E+00	8.9636E-03	0.0000E+00	7.8757E-06
		92235.60c	78774	5.5497E-01	8.6544E-02	4.0892E-01	5.7965E-06
		92238.60c	48898	3.6533E-01	8.6368E-02	7.0020E-04	1.9988E-05

The number of tritium atoms produced = reaction rate for ${}^6\text{Li}$. The reaction rate will then be calculated with the following equation:

$$Reaction\ rate = \frac{weight\ lost\ to\ capture}{collisions\ * weight} \times total\ collisions \quad (C. 1)$$

Similarly, we can calculate the energy produced, by calculating the reaction rate for ${}^{235}\text{U}$, considering that the fission makes about 85 % of the total reaction rate [4], because for thermal neutron ($\sigma_{\text{fission}} = 580$ barn and $\sigma_{\text{total}} = 678$ barn [4]). Also,

it is important to note that the energy released per fission of ^{235}U is about 200 MeV.

File output A: 20 cm thickness blanket – criticality summary box

```

-----
the final estimated combined collision/absorption/track-length keff = 0.99723 with an estimated standard deviation of 0.00301
the estimated 68, 95, & 99 percent keff confidence intervals are 0.99421 to 1.00024, 0.99123 to 1.00322, and 0.98927 to 1.00518
the final combined (col/abs/tl) prompt removal lifetime = 2.5225E-04 seconds with an estimated standard deviation of 1.7867E-06
-----

```

B.3 Verification ^6Li test output

Below is a portion taken from the output for ^6Li cross section test at $E = 0.3$ MeV.

```

1mcpn      version 4c      ld=01/20/00      02/20/23 20:39:56
*****
02/20/23 20:39:56      probid =
inp=test9C xsdir=xmdir1

1-      Controle test Li-6 in a 0.3 cm thick disk r=4cm, and E <= 300 keV
2-      c -----
3-      c < Cell Section >
4-      111  2  1.66692E-02  -10 -130 140      imp:n=1  $ Lithium-6
5-      113  0                -10 -140 180      imp:n=1  $ Lower void within the test cel
6-      114  0                -10 -170 130      imp:n=1  $ upper void within the test cel
7-      200  0                (10:170:-180)  imp:n=0  $ Outside world
8-
9-      c -----
10-     c < Surface Section >
11-     c The testing cell
12-     10      cz   4.0    $ The disk Radius
13-     c -----
14-     130     pz   5.3    $ Top surface of the disk
15-     140     pz   5.0    $ Bottom surface of the disk
16-     c -----
17-     170     pz  10.0    $ Top surface on the test cell
18-     180     pz   0.0    $ Bottom surface of the test cell
19-
20-     c -----
21-     c < Data Section >
22-     c Source Definition
23-     c Neutrons source
24-     c Monodirectional disk R=4 cm, Erg= 300 keV
25-     mode n
26-     sdef pos=0 0 3 AXS=0 0 1 EXT=0 RAD=d1 PAR=1 VEC=0 0 1 DIR=1 ERG=3e-1
warning. ext is constant. in most problems it is a variable.
27-     SI1 0 4
28-     SP1 -21 1
29-     nps 1e6
30-     c -----
31-     c m2 Lithium 6
32-     m2      3006.60c  -1.0  $ Li-6
33-     c -----

```

```

34-      c <Tallies>
35-      FC4   Three Bins Neutron Flux Tally in Li-6
36-      f4:n  111
37-      fm4   (-1 2 105)  $ 105 is the rxn to produce Tritium
38-      C SD4  1
39-      FC14  Four Group Neutron Flux Tally in Li-7
40-      f14:n 111
41-      E14   0.625e-6 2I 3e-1 $ Split flux to 4 groups 0 - 0.625 eV and up to 300 keV
42-      C SD14 1
43-      print 140
44-

```

1neutron activity of each nuclide in each cell, per source particle print table 140

cell	nuclides	atom fraction	total collisions	collisions * weight	weight lost to capture	weight gain by fission	weight gain by (n,xn)
1	111	3006.60c	1.0000E+00	31871	3.1459E-02	7.6336E-03	0.0000E+00
	total			31871	3.1459E-02	7.6336E-03	0.0000E+00
total over all cells for each nuclide			total collisions	collisions * weight	weight lost to capture	weight gain by fission	weight gain by (n,xn)
		3006.60c		31871	3.1459E-02	7.6336E-03	0.0000E+00

B. 4 Benchmarking with ORNL

A portion of the simplified ORNL verification file was presented including (table140).


```

1- MSR Based ON ORNL to creat Data Benchmarking.0.01 % Li-6 in Fuel, No blanket
2- c -----
3- c < Cell Section >
4- C 19 fuel pin, Reactor height 200 cm
5- c Fuel
6- 111 1 -3.05605 -10 u=1 imp:n=1 $ Fuel
7- 112 2 -1.75000 10 u=1 imp:n=1 $ Moderator (graphite)
8- c 113 2 -1.75000 11 u=1 imp:n=1 $ Moderator (graphite)
9- c Non-fuel element, ie moderator
10- 121 2 -1.75000 -10 u=2 imp:n=1 $ Empty cell, graphite
11- 122 2 -1.75000 10 u=2 imp:n=1 $ Empty cell, graphite
12- c 123 2 -1.75000 11 u=2 imp:n=1 $ Empty cell, graphite
13- c Lattice of universes 1 and 2
14- 500 0 -100 u=3 imp:n=1 lat=2
15- fill= -9:9 -9:9 0:0 $ Lattice
16- 2 2 2 2 2 2 2 2 2 2 2 2 2 2 2 2 2 2 2 2 2 2
17- 2 2 2 2 2 2 2 2 2 2 2 2 2 2 2 2 2 2 2 2 2 2
18- 2 2 2 2 2 2 2 2 2 2 2 2 2 2 2 2 2 2 2 2 2 2
19- 2 2 2 2 2 2 2 2 2 2 2 2 2 2 2 2 2 2 2 2 2 2
20- 2 2 2 2 2 2 2 2 2 2 2 2 2 2 2 2 2 2 2 2 2 2
21- 2 2 2 2 2 2 2 2 2 2 2 2 2 2 2 2 2 2 2 2 2 2
22- 2 2 2 2 2 2 2 2 2 2 2 2 2 2 2 2 2 2 2 2 2 2
23- 2 2 2 2 2 2 2 2 2 1 1 1 2 2 2 2 2 2 2 2 2 2
24- 2 2 2 2 2 2 2 2 2 1 1 1 1 2 2 2 2 2 2 2 2 2
25- 2 2 2 2 2 2 2 2 2 1 1 1 1 1 2 2 2 2 2 2 2 2
26- 2 2 2 2 2 2 2 2 2 1 1 1 1 2 2 2 2 2 2 2 2 2
27- 2 2 2 2 2 2 2 2 2 1 1 1 2 2 2 2 2 2 2 2 2 2
28- 2 2 2 2 2 2 2 2 2 2 2 2 2 2 2 2 2 2 2 2 2 2
29- 2 2 2 2 2 2 2 2 2 2 2 2 2 2 2 2 2 2 2 2 2 2
30- 2 2 2 2 2 2 2 2 2 2 2 2 2 2 2 2 2 2 2 2 2 2
31- 2 2 2 2 2 2 2 2 2 2 2 2 2 2 2 2 2 2 2 2 2 2
32- 2 2 2 2 2 2 2 2 2 2 2 2 2 2 2 2 2 2 2 2 2 2
33- 2 2 2 2 2 2 2 2 2 2 2 2 2 2 2 2 2 2 2 2 2 2
34- 2 2 2 2 2 2 2 2 2 2 2 2 2 2 2 2 2 2 2 2 2 2
35- 600 0 -300 -130 120 imp:n=1 fill=3 $ Core region with fuel
36- c 700 0 -400 -130 120 #600 imp:n=0 $ NO Blanket.
37- 1000 0 (300:130:-120) imp:n=0 $ Outside World
38-
39- c -----
40- c < Surface Section >
41- c Items in the hexcell
42- 10 cz 4.1 $ Fuel radius
43- c 11 cz 2.8 $ cladding, just graphite for now
44- c -----
45- c Hex cell
46- 100 rhp 0 0 -2 0 0 202 10.0 0 0
47- c 101 px 4.5 $ 1st side of the hexagonal lattice pin
48- c 102 2 px 4.5 $ 2nd side of the hexagonal lattice pin
49- c 103 3 px 4.5 $ 3rd side of the hexagonal lattice pin
50- c 104 4 px 4.5 $ 4th side of the hexagonal lattice pin
51- c 105 5 px 4.5 $ 5th side of the hexagonal lattice pin
52- c 106 6 px 4.5 $ 6th side of the hexagonal lattice pin
53- c -----
54- c The core
55- 120 pz 0.0 $ Bottom of core
56- 130 pz 200 $ Top of core
57- 300 cz 65 $ Core radius
58- c -----
59- c The blanket
60- c 140 pz -0.3 $ Bottom of blanket same as core
61- c 150 pz 150.3 $ Top of blanket same as core
62- c 400 cz 110 $ Radius, (outer radius)
63-
64- c -----

```

```

65- c < Data Section >
66- c Coordinate Transformation for lattice cell edges
67- c *TR2 0 0 0 60 30 90 150 60 90 90 90 0 1
68- c *TR3 0 0 0 120 30 90 150 120 90 90 90 0 1
69- c *TR4 0 0 0 180 90 90 90 180 90 90 90 0 1
70- c *TR5 0 0 0 120 150 90 30 120 90 90 90 0 1
71- c *TR6 0 0 0 60 150 90 30 60 90 90 90 0 1
72- c -----
73- c Source Definition
74- kcode 1000 1.0 30 150
75- sdef pos=0 0 75 $ Release 14 MeV neutrons somewhere in the middle.
76- mode n
77- totnu
78- c -----
79- c m1 Molten Salt fuel, 32% enrichment
80- m1 92235.60c -0.01633 $ U235, 32% enrichment
81- 92238.60c -0.03478 $ U238
82- 3006.60c -0.00001 $ Li-6
83- 3007.60c -0.10898 $ Li-7, 99.95% enrichment
84- 4009.60c -0.06274 $ Beryllium
85- 40000.60c -0.10900 $ Zirconium
86- 9019.60c -0.66816 $ Fluoride
87- c -----
88- c m2 is graphite moderator @ 300K *endf602*
89- m2 6000.60c -1.0 $ C
90- mt2 grph.01t $ Thermal Scattering
91- c -----
92- c m3 2LiF-BeF2 Blanket, No blanket
93- c m3 3006.60c -0.014730 $ Li-6, 10.55 % enrichment
94- c 3007.60c -0.124850 $ Li-7,
95- c 4009.60c -0.091103 $ Beryllium
96- c 9019.60c -0.769317 $ Fluoride
97- c -----
98- c <Tallies>
99- c FC4 Eight Group Neutron Flux Tally Fuel
100- c f4:n 600
101- c E4 0.625e-6 1e-6 1e-5 1e-4 1e-3 1 2.5 100 $ Split flux 8 groups
102- c SD4 1
103- c FC14 Four Bins Neutron Flux Tally in Blanket
104- c f14:n 600
105- c fm14 (-1 3 -2) (-1 3 16) (-1 3 105) (-1 3 91)
106- c SD14 1
107- print 140
108-

```

1neutron activity of each nuclide in each cell, per source particle print table 140

cell	nuclides	atom fraction	total collisions	collisions * weight	weight lost to capture	weight loss to fission	weight gain by (n,xn)	
1	111	92235.60c	1.1760E-03	76242	5.5029E-01	8.4004E-02	4.0908E-01	0.0000E+00
		92238.60c	2.4731E-03	24364	1.8501E-01	4.3437E-02	4.7515E-04	1.5059E-05
		3006.60c	2.8141E-05	2260	1.6217E-02	1.6106E-02	0.0000E+00	0.0000E+00
		3007.60c	2.6293E-01	174718	1.3744E+00	7.4833E-03	0.0000E+00	7.0892E-06
		4009.60c	1.1784E-01	351604	2.7263E+00	3.2601E-03	0.0000E+00	6.5854E-03
		40000.60c	2.0226E-02	81716	6.4155E-01	5.3462E-03	0.0000E+00	2.4820E-05
		9019.60c	5.9532E-01	1320197	1.0362E+01	8.8460E-03	0.0000E+00	0.0000E+00
		total		16461605	1.2777E+02	1.9156E-01	4.0956E-01	6.6323E-03
total over all cells for each nuclide			total collisions	collisions * weight	weight lost to capture	weight loss to fission	weight gain by (n,xn)	
	3006.60c		2260	1.6217E-02	1.6106E-02	0.0000E+00	0.0000E+00	
	3007.60c		174718	1.3744E+00	7.4833E-03	0.0000E+00	7.0892E-06	
	4009.60c		351604	2.7263E+00	3.2601E-03	0.0000E+00	6.5854E-03	
	6000.60c		14430504	1.1192E+02	2.3076E-02	0.0000E+00	0.0000E+00	
	9019.60c		1320197	1.0362E+01	8.8460E-03	0.0000E+00	0.0000E+00	
	40000.60c		81716	6.4155E-01	5.3462E-03	0.0000E+00	2.4820E-05	
	92235.60c		76242	5.5029E-01	8.4004E-02	4.0908E-01	0.0000E+00	
	92238.60c		24364	1.8501E-01	4.3437E-02	4.7515E-04	1.5059E-05	

the final estimated combined collision/absorption/track-length keff = 0.99812 with an estimated standard deviation of 0.00299
the estimated 68, 95, & 99 percent keff confidence intervals are 0.99513 to 1.00111, 0.99216 to 1.00407, and 0.99022 to 1.00602
the final combined (col/abs/tl) prompt removal lifetime = 3.6364E-04 seconds with an estimated standard deviation of 2.1789E-06

Appendix C Useful Constants, and Useful Mathematics

C.1 Constants, Masses and Conversion factors

Constants:

Speed of light	c	2.997924582×10^8 m/s
Charge of electron	e	1.602189×10^{-19} C
Boltzmann constant	k_B	1.38066×10^{-23} J/K
		8.61740×10^{-5} eV/K
Plank's constant	h	6.62618×10^{-34} J . s
		4.13570×10^{-15} eV . s
		$\hbar = h/2\pi$
		1.054589×10^{-34} J . s
		6.582170×10^{-16} eV . s
Avogadro's number	N_A	6.022045×10^{23} mole ⁻¹
Fine structure constant	hc	1239.853 MeV . fm
	$\hbar c$	197.329 MeV . fm
	$e^2/4\pi\epsilon_0$	1.4339976 MeV . fm

Particle rest mass:

	u	MeV / c^2
Electron	5.485803×10^{-4}	0.511003
Proton	1.00727647	938.280
Neutron	1.00866501	939.573
Deuteron	2.01355321	1875.628
Alpha	4.00150618	3727.409

Conversion Factors:

$$1 \text{ eV} = 1.602189 \times 10^{-19} \text{ J}$$

$$1 \text{ barn} = 10^{-28} \text{ m}^2$$

$$1 \text{ Ci} = 3.7 \times 10^{10} \text{ decays/s}$$

$$1 \text{ u} = 931.502 \text{ MeV}/c^2 = 1.660566 \times 10^{-27} \text{ kg}$$

C. 2 Maxwell-Boltzmann Distribution

In a gas like system of particle at a fixed temperature T , the energy/or speed of the individual particles is not constant, but distributed according to *Maxwell-Boltzmann* distribution, which gives the probability that a given particle has an energy E or a speed v . The probability distribution is given by equation (D. 1) [11]-(Sec 4.6).

$$P(E) \propto \exp(-E/k_B T) \tag{D. 1}$$

Where the term $\exp(-E/k_B T)$ is known as the (Boltzmann factor). Maxwell-Boltzmann is the speed distribution function which gives the fraction of particles of mass m with velocities between v and $v + dv$ according to equation 1.46), and illustrated in **Error! Reference source not found.**

Thus, to get the average value of energy, the average value of speed should be calculated according to equation.

$$\langle v^2 \rangle = \int_0^\infty v^2 f(v) dv = \frac{3k_B T}{m} \rightarrow \langle E \rangle = \frac{1}{2} m \langle v^2 \rangle = \frac{3}{2} k_B T \tag{D. 2}$$

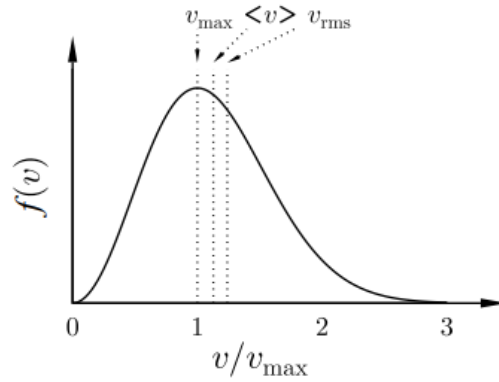


Figure C. 1. Speed distribution function (Maxwell-Boltzmann distribution) [11]-
(Sec 5.2)

C. 3 Useful Mathematics

Integrals [11]:

$$\int_0^{\infty} x^2 \exp(-cx^2) dx = \frac{1}{4} \sqrt{\frac{\pi}{c^3}}$$

$$\int_0^{\infty} x^3 \exp(-cx^2) dx = \frac{1}{2c^2}$$

$$\int_0^{\infty} x^4 \exp(-cx^2) dx = \frac{3}{8} \sqrt{\frac{\pi}{c^5}}$$

Dirac delta function [11]:

Denoted $\delta(x - c)$ is a function that is zero everywhere except $x = c$, with area = 1:

$$\int_{-\infty}^{\infty} \delta(x - a) = 1$$

References

- [1] R. J. Pearson, A. B. Antoniazzi and W. J. Nuttall, "Tritium supply and use: a key issue for the development of nuclear fusion," *Fusion Engineering and Design*, vol. 136 Part B, pp. 1140 - 1148,, 2018. [Online]. Available: <https://doi.org/10.1016/j.fusengdes.2018.04.090>.
- [2] "International Thermonuclear Experimental Reactor," ITER, [Online]. Available: <https://www.iter.org/> . [Accessed 14 July 2022].
- [3] B. R. Martin and S. Graham, *NUCLEAR AND PARTICLE PHYSICS - AN INTRODUCTION*, WILEY, 2019.
- [4] J. R. Lamarsh, *Introduction to NUCLEAR REACTOR THEORY*, American Nuclear Society, Inc., 2002.
- [5] K. S. Krane, *INTRODUCTORY NUCLEAR PHYSICS*, WILEY, 1988.
- [6] G. R. Longhurst, K. Tsuchiya, C. H. Dorn, S. L. Folkman, T. H. Fronk, M. Ishihara, H. Kawamura and T. N. Tranter, "Managing Beryllium in Nuclear Facility Applications," *Taylor and Francis Online - Nuclear Technology*. DOI: 10.13182/NT11-A13318, vol. 176, no. 3, pp. 430-441, 10 Apr 2017.
- [7] NNDC, "Evaluated Nuclear Data File," National Nuclear Data Center, [Online]. Available: <https://www.nndc.bnl.gov/ndf/>.

- [8] D. Holcomb, United States Nuclear Regulatory Commission, 08 November 2017. [Online]. Available:
<https://www.nrc.gov/docs/ML1733/ML17331B113.pdf>.
- [9] A. Piel, Plasma Physics - An Introduction to Laboratory, Space, and Fusion Plasmas - Second Edition, Springer, 2017.
- [10] "Euro-Fusion," [Online]. Available: <https://euro-fusion.org/fusion/fusion-on-the-sun/>. [Accessed 20 October 2022].
- [11] S. J. Blundell and K. M. Blundell, Concepts in Thermal Physics, Second Edition: OXFORD, 2010.
- [12] "JET: the Joint European Torus," UK Atomic Energy Authority, [Online]. Available: <https://ccfe.ukaea.uk/research/joint-european-torus/>. [Accessed 14 July 2022].
- [13] C. Osolin, J. Kawamoto, ., B. Evangelista and A. Chen, "REACHING THE THRESHOLD OF IGNITION," Lawrence Livermore National Laboratory, [Online]. Available:
<https://lasers.llnl.gov/content/assets/docs/news/reaching-the-threshold-of-ignition-magazine.pdf>. [Accessed 20 June 2022].
- [14] J. Owen, J. R. Pasley and C. P. Ridgers, "Investigation of the performance of mid-Z hohlraum wall liners for producing X-ray drive," AIP Publishing

<https://doi.org/10.1063/5.0029689>, 2021.

- [15] INFO-0793, "Tritium Releases and Dose Consequences in Canada in 2006," Canadian Nuclear Safety Commission (CNSC), 2009.
- [16] M. Rubel, "Fusion Neutrons: Tritium Breeding and Impact on Wall Materials and Components of Diagnostic Systems," *Journal of Fusion Energy*, vol. 38, no. <https://doi.org/10.1007/s10894-018-0182-1>, p. 315–329, 2019.
- [17] D. McMorrow, "Tritium JSR-11-345," The MITRE Corporation, McLean, Virginia 2210, 2011.
- [18] Sara E. Ferry, Kevin B. Woller, Ethan E. Peterson,, Caroline Sorensen and Dennis G. Whyte, "The LIBRA Experiment: Investigating Robust Tritium Accountancy in Molten FLiBe Exposed to a D-T Fusion Neutron Spectrum," *Fusion Science and Technology*, vol. 79, no. 1, pp. 13 - 35, 2022.
- [19] B.N. Sorbom, J. Ball, T.R. Palmer, F.J. Mangiarotti, D.G. Whyte, C. Kasten, D.A. Sutherland, H.S. Barnard, C.B. Haakonsen and J. Goh, "ARC: A compact, high-field, fusion nuclear science facility and demonstration power plant with demountable magnets," *Fusion Engineering and Design*, vol. 100, no. <https://doi.org/10.1016/j.fusengdes.2015.07.008>, pp. 378 -

405, 2015.

- [20] Xiaoyu WANG, Kaiming Feng, Y.J. Chen, long zhang, Y.J. Feng, Xinghua Wu, hongbin liao, Xingfu Ye, Fengchao Zhao and Qixiang Cao, "Current design and R&D progress of the Chinese helium cooled ceramic breeder test blanket system," *IOPScience Nuclear Fusion*, vol. 59 Number 7, no. DOI 10.1088/1741-4326/ab0c32, 2019.
- [21] Jacob Fantidis, D.V. Bandekas, Constantinos Potolias and N. Vordos, "Fast and thermal neutron radiographies based on a compact neutron generator," *Journal of Theoretical and Applied Physics*, no. <https://doi.org/10.1186/2251-7235-6-20>, 2012.
- [22] "ORNL - 4812 The Development Status of Molten-Salt Breeder Reactors," Oak Ridge National Laboratory, 1972.
- [23] J. H. Shaffer, "ORNL - 4616 PREPARATION AND HANDLING OF SALT MIXTURES FOR THE MOLTEN SALT REACTOR EXPERIMENT," Oak Ridge National Laboratory, 1971.
- [24] S. Guo, J. Zhang, W. Wu and Z. Zhou, "Corrosion in the molten fluoride and chloride salts and materials development for nuclear applications," *ELSEVIER/Progress in Materials Science*, vol. 97, no. <https://doi.org/10.1016/j.pmatsci.2018.05.003>, pp. 448 - 487, 2018.

- [25] D. F. Williams, L. M. Toth and K. T. Clarno , "ORNL/TM-2006/12 Assessment of Candidate Molten Salt Coolants for the Advanced High-Temperature Reactor (AHTR)," OAK RIDGE NATIONAL LABORATORY , 2006.
- [26] L. Vergari, R. O. Scarlat, R. D. Hayes and M. Fratoni, "The corrosion effects of neutron activation of 2LiF-BeF₂ (FLiBe)," *ELSEVIER/Nuclear Materials and Energy*, vol. 34, no. <https://doi.org/10.1016/j.nme.2022.101289>, 2022.
- [27] Manual, MCNP4C: Monte Carlo N-Particle Transport Code System., Los Alamos National Laboratory, April, 2000.
- [28] G. T. Mays, A. N. Smith and J. R. Engel, "ORNL/TM-5759 Distribution and Behavior of Tritium in the Coolant-Salt Technology Facility," Oak Ridge National Laboratory, 1977.
- [29] "Britannica," [Online]. Available: <https://www.britannica.com/science/periodic-table>.
- [30] "International Atomic Energy Agency," [Online]. Available: <https://www.iaea.org/>.